A GABAergic Tecto–Tegmento–Tectal Pathway in Pigeons

Martin Stacho,[1]* Sara Letzner,[1] Carsten Theiss,[2] Martina Manns,[1] and Onur Güntürkün[1]

[1]Department of Biopsychology, Faculty of Psychology, Institute of Cogntive Neuroscience, Ruhr-University Bochum, 44801 Bochum, Germany

[2]Department of Cytology, Faculty of Medicine, Ruhr-University Bochum, 44801 Bochum, Germany

ABSTRACT

Previous studies have demonstrated that the optic tecta of the left and right brain halves reciprocally inhibit each other in birds. In mammals, the superior colliculus receives inhibitory γ-aminobutyric acid (GABA)ergic input from the basal ganglia via both the ipsilateral and the contralateral substantia nigra pars reticulata (SNr). This contralateral SNr projection is important in intertectal inhibition. Because the basal ganglia are evolutionarily conserved, the tectal projections of the SNr may show a similar pattern in birds. Therefore, the SNr could be a relay station in an indirect tecto–tectal pathway constituting the neuronal substrate for the tecto–tectal inhibition. To test this hypothesis, we performed bilateral anterograde and retrograde tectal tracing combined with GABA immunohistochemistry in pigeons. Suprisingly, the SNr has only ipsilateral projections to the optic tectum, and these are non-GABAergic. Inhibitory GABAergic input to the contralateral optic tectum arises instead from a nearby tegmental region that receives input from the ipsilateral optic tectum. Thus, a disynaptic pathway exists that possibly constitutes the anatomical substrate for the inhibitory tecto–tectal interaction. This pathway likely plays an important role in attentional switches between the laterally placed eyes of birds. J. Comp. Neurol. 000:000–000, 2016.

INDEXING TERMS: substantia nigra; tecto–tectal interaction; nucleus of the lateral ponto-mesencephalic tegmentum; retrograde and anterograde tracing; GABA; parvalbumin; RRIDs: AB_211712; AB_258833; AB_2201526; AB_477652; AB_477329; SciRes_000111

The optic tectum (TeO) is a phylogenetically old, paired midbrain structure that is present in all vertebrates. It encapsulates the torus semicircularis, sometimes called the tectum acusticum. Because the tectum opticum and torus semicircularis assume separate locations along the longitudinal axis of the brainstem in mammals, the mammalian TeO is called the superior colliculus (SC). The laminated appearance and general connectivity pattern of the TeO are similar across taxa (Grofová et al., 1978; Grover and Sharma, 1981; Northcutt, 1982; Lázár et al., 1983; Welker et al., 1983; Huerta and Harting, 1984; Luksch, 2003; Hellmann et al., 2004). The vertebrate TeO is an essential relay station for visuomotor transformation and plays a crucial role in saccadic eye movements, prey-catching, spatial attention, and stimulus selection (Sparks and Mays, 1990; Ewert et al., 1999, 2001; Luque et al., 2005; Wurtz, 2009; Knudsen, 2011; Mysore and Knudsen, 2011; Krauzlis et al., 2013). The left and right TeO modulate their activity patterns via the tectal (CT) and the posterior commissures (CP) (Robert and Cuénod, 1969a,b; Niida, 1973; Mascetti and Arriagada, 1981; Rhoades et al., 1981, 1986; Keysers et al., 2000). These commissures have been implicated in interhemispheric transfer of visual discriminations in fish (Mark, 1966; Ingle and Campbell, 1977; Hemsley and Savage, 1989), in transfer of habituated stimuli and in lateralized visuomotor behavior in birds (Hamassaki and Britto, 1987; Güntürkün and Böhringer, 1987), and in transfer of black–white discrimination, recovery from cortical hemianopia, and to some extent transfer of motion and brightness discrimination in mammals

Grant sponsor: German Research Foundation (DFG); Grant numbers: SFB864 and MA4485/1 and MA4485.2 (to M.M.).

*CORRESPONDENCE TO: Martin Stacho, Ruhr-University Bochum, Institute of Cognitive Neurosciences, Faculty of Psychology, Department of Biopsychology, Universitätstraße 150, 44801 Bochum, Germany.
E-mail: Martin.Stacho@rub.de

Received November 24, 2015; Revised March 10, 2016;
Accepted March 10, 2016.
DOI 10.1002/cne.23999
Published online Month 00, 2016 in Wiley Online Library (wileyonlinelibrary.com)

(Sherman, 1974; Peck et al., 1979; Hottman, 1981; Sprague, 1991).

However, it seems that only a small fraction of CT/CP is constituted by direct tecto–tectal fibers (fish: Grover and Sharma, 1981; Smeets, 1981; Northcutt, 1982; Herrero et al., 1999; amphibians: Wilczynski and Northcutt, 1977; Lázár, 1984; mammals: Edwards, 1977; Yamasaki et al., 1984; Chebat et al., 2006; Tardif and Clarke, 2002; reptiles: Gruberg et al., 1979; Welker et al., 1983; Northcutt, 1984; Pérez-Santana et al., 1996; birds: Voneida and Mello, 1975; Hunt and Künzle, 1976). Instead, these studies indicate that the majority of commissural fibers interconnect the TeO with the contralateral tegmentum and pretectum. Thus, the intertectal interaction is possibly more strongly mediated via polysynaptic pathways than via direct monosynaptic tecto–tectal connections (Robert and Cuénod, 1969a,b; Hardy et al., 1984). In accordance, studies in mammals have showm that projections of the substantia nigra pars reticulata (SNr), which run via the CT to the contralateral SC (Bickford and Hall, 1992), could modulate interhemispheric transfer (Wallace et al., 1989, 1990; Sprague, 1991). Therefore, the SNr might be an important relay station in tecto–tectal communication. The SNr is an output structure of the basal ganglia and exerts bilateral inhibition on the SC (Rinvik et al., 1976; Grofová et al., 1978; Beckstead and Frankfurter, 1982; Gerfen et al., 1982; Araki et al., 1984; May and Hall, 1986; Harting et al., 1988; Bickford and Hall, 1992; Deniau and Chevalier, 1992; Liu and Basso, 2008). The basal-ganglionic outflow to the TeO via the SNr is a conserved vertebrate feature (Reiner et al., 1998; Stephenson-Jones et al., 2012).

Up to now the pathways via which the two tecta interact in birds has been unclear. Based on the demonstration of contralateral SNr–SC projections in mammals and their relation to interhemispheric transfer, we assumed that also in birds the SNr could constitute an important relay station in tecto–tectal communication. Using bilateral tectal antero- and retrograde tracing and γ-aminobutyric acid (GABA) and parvalbumin (PV) immunohistochemistry, we aimed to uncover a tecto–SNr–tectal pathway in pigeons, which could constitute the anatomical substrate for the inhibitory interactions between the left and the right TeO.

MATERIALS AND METHODS

Animals

In total 49 homing pigeons (*Columba livia*) of both sexes from local breeding stocks were used in this study. To demonstrate a disynaptic pathway between

Abbreviations

ACSF	artificial cerebrospinal fluid
AD	dorsal arcopallium
AI	intermediate arcopallium
AL	ansa lenticularis
BCA	brachium conjunctivum ascendens
BCD	brachium conjunctivum descendens
BCS	brachium colliculi superioris
BDA	biotinylated dextran amine
CDL	area corticoidea dorsolateralis
CP	posterior commissure
CT	tectal commissure
CTB	cholera toxin subunit B
DIP	dorsointermediate posterior thalamic nucleus
dITPO	dorsolateral part of the temporo–parieto–occipital area
DLP	dorsolateral posterior thalamic nucleus
DMP	dorsomedial posterior thalamic nucleus
E	entopallium
EW	Edinger–Westphal nucleus
FLM	medial longitudinal fascicle
FPL	lateral forebrain bundle
FRL	lateral reticular formation
GABA	γ -aminobutyric acid
GP	globus pallidus
HA	hyperpallium apicale
HD	hyperpallium dorsale
HI	hyperpallium intercalatum
HP	hippocampus
ICo	nucleus intercollicularis
Imc	isthmic nucleus pars magnocellularis
ION	isthmo-optic nucleus
Ipc	isthmic nucleus pars parvocellularis
IPS	interstitio–pretecto–subpretectal nucleus
IS	incubation solution
L	layer
LAD	lamina arcopallialis dorsalis
LFM	lamina frontalis suprema
LFS	lamina frontalis superior
LM	lamina mesopallialis
LoC	locus coeruleus
LSt	lateral striatum
M	mesopallium
MLd	lateral mesencephalic nucleus pars dorsalis
MSt	medial striatum
MW	molecular weight
N	nidopallium
nLPT	nucleus of the lateral ponto-mesencephalic tegmentum
nOM	nucleus nervi oculomotorii
nSP	subpretectal nucleus
nTT	nucleus of the tecto–thalamic tract
nIV	nucleus nervi trochlearis
OM	occipito–mesencephalic tract
OMv	ventral oculomotor nucleus
PBS	phosphate-buffered saline
PST	pretecto–subpretectal tract
PT	pretectal nucleus
PV	parvalbumin
Rt	nucleus rotundus of the thalamus
SC	superior colliculus
SCE	stratum cellulare externum
SLu	nucleus semilunaris
SNc	substantia nigra pars compacta
SNr	substantia nigra pars reticulata
SpL	lateral spiriform nucleus
SpM	medial spiriform nucleus
SRt	subrotundal nucleus
STN	subthalamic nucleus
TDA	Texas red dextran amine
TeO	optic tectum
Th	thalamus
TnA	nucleus taeniae of the amygdala
TP	tecto–pontine tract
TPO	temporo–parieto–occipital area
V	ventricle
VIA	ventrointermediate nucleus of the thalamus
VP	ventral pallidum

the optic tecta, seven animals were bilaterally injected with two different tracers into the left and right TeO, respectively. From these seven animals, two pigeons were injected with cholera toxin subunit B (CTB; Sigma, Hamburg, Germany) into the left or right TeO and with biotinylated dextran amine (BDA; 10,000 molecular weight [MW]; Invitrogen, Darmstadt, Germany) into the contralateral side. One animal was injected with CTB and BDA (3,000 MW; Invitrogen) into the right and left TeO, respectively. Four animals received Texas red dextran amine (TDA; 10, 000 MW; Invitrogen) into the left or right TeO and CTB or BDA (10,000 MW) into the contralateral TeO. Furthermore, two animals received multiple unilateral injections of CTB into the TeO distributed along the almost complete rostrocaudal and dorsoventral tectal axis to visualize all possible tectal afferents. To investigate the topography of the tegmental relay stations, four animals received unilateral CTB and TDA injections into either the dorsal and ventral or rostral and caudal TeO. Thirty animals were used for unilateral injections of either CTB or BDA (10,000 MW; Invitrogen) into the lateral tegmentum. A further six animals were injected with BDA (3000 MW) or biocytin (Santa Cruz Biotechnology, Santa Cruz, CA) into the lateral tegmentum in vitro. These injections aimed to reveal the layer-specific origins of afferents and terminations of efferents of the tegmental relay station.

All procedures were in compliance with the U.S. National Institutes of Health guidelines for laboratory animals and were approved by the National Committee of North Rhine-Westphalia, Germany.

Surgical procedure and in vivo injections

The animals were anesthetized with either a mixture (7:3; 0.15 ml/100 g body weight) of ketamine (100 mg/ml; Zoetis, Berlin, Germany) and xylazine (20 mg/ml; Bayer Vital, Leverkusen, Germany) or with isoflurane (0.5–5%; AbbVie Deutschland, Ludwigshafen am Rhein, Germany). Pigeons anesthetized with isoflurane received 0.2 ml Dolorex (10 mg/ml; Intervet Deutschland, Unterschleissheim, Germany) 10 minutes before anesthesia. The anesthetized animals were positioned in a stereotaxic apparatus, and their heads were fixed in either a lateral or frontal head-holder. Feathers on the head were cut, and the scalp was incised to expose the skull. The surrounding muscles were carefully pulled aside when needed, and the cranial bone was opened above the injection site using an electric drill. The meninges were opened, and a glass micropipette (15–20-µm inner diameter) filled with the appropriate tracer was lowered into the brain tissue. Because the topography of the avian nigrotectal and tectonigral projections were unknown, tectal injections were made at multiple sites along the whole anterior–posterior and dorsal–ventral axes ranging from four to eight injection sites in total. All tectal injections were made at 1-mm and 0.5-mm depth. At each injection site, 100 nl of the tracer was applied at each depth using a mechanic pressure device (Nanoliter injector 2000; WPI, Berlin, Germany). In case of bilateral tracings, injections of dextran amines (TDA or BDA) were made first, followed by CTB injections 5 days later during a separate surgery. Tegmental injections were placed anterior between 3.25 and 1.50, lateral at 3.00, and about 5 mm deep under the dorsal surface of the tectum (Karten and Hodos, 1967). These injections were made either via the cerebellum or via the mediodorsal or ventrolateral tectum.

After 2 days of survival (CTB injections) and/or 7 days after BDA or TDA injections, the animals were deeply anesthetized with Equithesin (0.45 ml/100 g body weight) and perfused transcardially with 0.9% NaCl followed by cooled (4 °C) 4% paraformaldehyde in 0.12 M phosphate buffer (PB; pH 7.4). The brains were dissected and postfixed in 4% paraformaldehyde/30% sucrose in PB solution at 4 °C for 2 hours. Subsequently, the brains were cryoprotected in 30% sucrose solution in phosphate-buffered saline (PBS; pH 7.4) for 24 hours. To facilitate slicing, brains were embedded in 15% gelatin/30% sucrose and were further fixated in 4% paraformaldehyde in PBS for 24 hours. Brains were cut in the coronal plane in 30-µm-thick slices using a freezing microtome (Leica, Wetzlar, Germany) and stored at 4 °C in 0.1% sodium azide until further processing. Every 10th slice was used for one staining.

In vitro injections

For in vitro tracing, the animals were either directly decapitated or first anesthetized with Equithesin (0.45 ml/100 g body weight) and perfused with an ice-cooled sucrose-substituted Krebs solution (210 mM sucrose, 3 mM KCl, 3 mM $MgCl_2{\cdot}6H_2O_2$, 23 mM $NaHCO_3$, 1.2 mM $NaH_2PO_4{\cdot}H_2O$, 11 mM β-D-glucose). The brains were quickly dissected and then submerged in this solution for 2 minutes. The brains were then blocked in 1.65% agar diluted in 4-(2-hydroxyethyl)piperazine-1-ethanesulfonic acid (HEPES) solution (290 mM sucrose, 3 mM KCl, 3 mM $MgCl_2.6H_2O_2$, 5 mM HEPES) and cut into 500–1,000-µm-thick coronal slices with a vibratome (Leica VT 1000S). The slices were collected in artificial cerebrospinal fluid (ACSF; 120 mM NaCl, 3 mM KCl, 1 mM $MgCl_2{\cdot}6H_2O_2$, 23 mM $NaHCO_3$, 1.2 mM $NaH_2PO_4{\cdot}H_2O$, 2 mM $CaCl_2{\cdot}2H_2O$, 11 mM β-D-glucose) continuously oxygenized with carbogen (95% O_2/5% CO_2) at room temperature. For injections, the sections were placed in a chamber containing ACSF and injected with 50–100 nl of BDA (3,000 MW) or biocytin (Santa

TABLE 1.
Primary Antibodies Used

Antigen	Immunogen	Manufacturer, cat. no., RRID; species, poly/monoclonal	Dilution
Cholera toxin subunit B (CTB)	Nondenatured CTB isolated from *Vibria cholerae*	EMD Millipore, cat. no. 227040-100UL, RRID: AB_211712; goat, polyclonal	1:20,000; 1:10,000; 1:1,000
Cholera toxin subunit B	Nondenatured CTB isolated from *Vibria cholerae*	Sigma-Aldrich, cat. no. C3062, RRID: AB_258833; rabbit, polyclonal	1:5,000; 1:1,000
Tyrosine hydroxylase	Purified tyrosinehydroxylase from ratpheochromocytoma	Millipore, cat. no. MAB5280, RRID: AB_2201526; mouse, monoclonal	1:2,000
γ-Aminobutyric acid (GABA)	GABA conjugated to bovine serum albumin	Sigma-Aldrich, cat. no. A2052, RRID: AB_477652; rabbit, polyclonal	1:1,000
Parvalbumin	Purified frog muscle parvalbumin	Sigma-Aldrich, cat. no. P3088, RRID: AB_477329; mouse, monoclonal	1:2,000

Cruz Biotechnology) using a glass micropipette (20-μm inner diameter). The slices were kept in the continuously carbogenized ACSF for 4–22 hours at room temperature and were thereafter immersed in 4% paraformaldehyde in 0.12 M PB (pH 7.4) for 12 hours. Subsequently, they were cryoprotected in 30% sucrose solution (in PBS; pH 7.4) until they had sunk, and were then resectioned on a freezing microtome (Leica) into 35-μm-thick slices. The slices were further processed according to the 3,3′-diaminobenzidine tetrahydrochloride (DAB) protocol described below.

Immunohistochemistry

For a list of the primary antibodies used, see Table 1.

CTB, BDA, and biocytin visualization with DAB

CTB, BDA, and biocytin were visualized using a standard DAB staining procedure intensified with nickel and cobalt (Shu et al, 1998; Hellman and Güntürkün, 2001). The slices were rinsed in PBS (3 × 10 minutes) and incubated in 0.3% hydrogen peroxide (H_2O_2) in distilled water for 30 minutes to block endogenous peroxidases. After further rinsing (3 × 10 minutes in PBS), BDA- and biocytin-injected slices were directly incubated in the avidin–biotin–peroxidase complex (ABC; see below), whereas the CTB slices were incubated in 10% normal rabbit serum (NRS; Vectastain Elite ABC kit, Vector, Burlingame, CA) in PBS with 0.3% Triton-X-100 (PBST) to block nonspecific binding sites. After rinsing in PBS for 5 minutes, slices were incubated in a polyclonal goat anti-CTB antibody (EMD Millipore, Darmstadt, Germany, cat. no. 227040-100UL; RRID: AB_211712) at a concentration of 1:20,000 (1:10,000 when counterstained with Nissl) at 4 °C for 1–3 days. After rinsing in PBS (3 × 10 minutes), slices were transferred into secondary biotinylated rabbit anti-goat antibody (1:200 in PBST; Vectastain Elite ABC kit, Vector) for 60 minutes at room temperature. After further washing in PBS (3 × 10 minutes), slices were incubated in ABC (Vectastain Elite ABC kit, Vector; 1:100 in PBST) for 60 minutes at room temperature. Slices were rinsed 3 × 10 minutes in PBS, 1 × 5 minutes in 0.1 M sodium acetate buffer (pH 6.0), and then transferred into a DAB solution, containing β-D-glucose, for visualization. The staining reaction was induced by adding glucose–oxidase (80–100 μl in 50 ml DAB solution). The reaction lasted 30 minutes (staining intensity was visually controlled), and the reaction solution was changed every 10 minutes. Rinsing the slices in 0.1 M sodium acetate buffer (pH 6.0; 3 × 5 minutes) stopped the reaction. After washing in PBS (3 × 10 minutes), slices were mounted on gelatin-coated slides and either counterstained with Nissl or directly dehydrated in ethanol and coverslipped with DPX (Fluka, Munich, Germany).

CTB–BDA fluorescence double staining

Fluorescence CTB–BDA double staining was used to demonstrate anterogradely labeled fibers and retrogradely labeled neurons within the same sections. Slices were washed in PBS before (3 × 10 minutes) and after (1 × 5 minutes) incubation in 10% normal goat serum (30 minutes; Vectastain Elite ABC kit, Vector; in PBST). Then they were incubated in a polyclonal rabbit anti-CTB antibody (Sigma-Aldrich, Steinheim, Germany, cat. no. C3062; RRID: AB_258833; 1:5,000 in PBST) overnight. The next day, the slices were washed in PBS (3 × 10 minutes) and incubated in a mixture of the secondary antibody Alexa 488 donkey anti-rabbit (Invitrogen; 1:1,000 in PBST) and Alexa 594 streptavidin (Invitrogen; 1:1,000 in PBST) for 60 minutes. Streptavidin, like avidin, binds strongly to biotin and therefore can be used to visualize BDA, if conjugated to a fluorophore. Finally, the slices were washed in PBS (3 × 10 minutes), mounted on polarized glass slides, and coverslipped with Fluoromount (SouthernBiotech, Birmingham, AL).

CTB–tyrosine hydroxylase fluorescence double staining

For CTB–tyrosine hydroxylase (TH) double staining, the slices were washed 3 × 10 minutes in PBS and

incubated in 10% normal goat serum (in PBST) for 30 minutes (Vectastain Elite ABC kit, Vector). After further washing (1 × 5 minutes), they were incubated in a mixture of polyclonal rabbit anti-CTB antibody (Sigma-Aldrich, cat. no. C3062; RRID: AB_258833; 1:1,000 in PBST) and monoclonal mouse anti-TH antibody (Millipore, cat. no. MAB5280; RRID: AB_2201526; 1:2,000 in PBST) for 72 hours. After 3 days, the slices were washed in PBS (3 × 10 minutes) and incubated in a mixture of secondary antibodies consisting of Alexa 488 goat anti-rabbit (Invitrogen; 1:200 in PBST) and Alexa 594 goat anti-mouse (Invitrogen; 1:200 in PBST) for 60 minutes. After washing for 3 × 10 minutes in PBS, the slices were mounted on polarized glass slides and coverslipped with Fluoromount (SouthernBiotech).

GABA staining

For GABA staining, the slices were washed in PBS (3 × 10 minutes) and then incubated in a polyclonal rabbit anti-GABA antibody (Sigma-Aldrich, cat. no. A2052; RRID: AB_477652; 1:1,000) diluted 1:1,000 in the incubation solution (IS; consisting of 2% NaCl, 0.3% Triton, 4% BSA in 0.05 M Tris-buffered saline) with 5% normal goat serum (Vectastain Elite ABC kit, Vector) for 3 days. Subsequently, the slices were washed in PBS (3 × 10 minutes) and incubated in the secondary Alexa 488 goat anti-rabbit antibody (1:500 in IS) with 5% normal goat serum for 1 hour. After washing (3 × 10 minutes in PBS) the primary reaction was repeated again for 1 day. On the next day the secondary reaction was repeated, and the slices were mounted on polarized glass slides and coverslipped with Fluoromount (SouthernBiotech).

GABA–CTB double staining

When GABA staining was combined with CTB labeling, the CTB staining was completed before GABA staining. In both CTB and GABA protocols, normal horse serum (Vectastain Elite ABC kit, Vector) was used. The CTB staining was performed as described in the CTB–TH double staining except that the polyclonal goat anti-CTB antibody (EMD Millipore, cat. no. 227040-100UL; RRID: AB_211712; 1:1,000 in PBST) was used as the primary and Alexa 594 donkey anti-goat (Invitrogen; 1:200 in PBST) as the secondary antibody. The GABA staining was performed as described in the previous paragraph but with Alexa 488 donkey anti-rabbit (Invitrogen; 1:500 in IS) as the secondary antibody.

Parvalbumin staining

For PV staining, the slices were washed in PBS (3 × 10 minutes) and then incubated in 10% normal goat serum (Vectastain Elite ABC kit, Vector; in PBST) for 30 minutes. After 5 minutes of washing in PBS, they were incubated in monoclonal primary mouse anti-PV antibody (Sigma-Aldrich, cat. no. P3088; RRID: AB_477329; 1:2,000 in PBST) for 3 days. After washing (3 × 10 minutes in PBS), slices were incubated in the secondary antibody. If the PV staining was combined with TDA, the secondary Alexa 488 goat anti-mouse antibody (Invitrogen; 1:200 in PBST) was used. In the case of CTB–PV or PV–GABA double staining, the secondary Alexa 594 goat anti-mouse antibody (Invitrogen; 1:200 in PBST) was used. The CTB–PV double staining was performed in parallel similar to CTB–TH double staining, whereas PV–GABA double staining was performed successively, with PV first and GABA staining second.

Histological analysis

The microscopic analysis was performed with a Zeiss (Oberkochen, Germany) Imager.M1 AXIO equipped with an AxioCam MRm Zeiss 60N-C 2/3" 0.63 × camera. The fluorescent slices were analyzed with Zeiss filter sets 45 (excitation: BP 560/40, beam splitter: FT 585, emission: BP 630/75) and 38 (excitation: BP 470/40, beam splitter: FT 495, emission: BP 525/50). The computer software AxioVision (AxioVision, Zeiss; RRID: SciRes_000111; version 4.8.1.0) was used for taking photographs of the relevant slices as well as for adjusting color balance, contrast, and brightness. Confocal analysis was performed with the aid of a confocal laser scanning microscope (LSM 510, Zeiss) in combination with Zeiss 40 × (Plan-Neofluar, NA 1.3) oil immersion lenses. The figures were prepared in CorelDRAW X5 (Version 15.2.0.686; Corel, Ottawa, ON, Canada).

RESULTS

The aim of this study was the identification of the indirect disynaptic connection between the left and the right TeO in pigeons, which could constitute an important pathway for inhibitory tecto–tectal interactions. We hypothesized that the SNr could be the main tegmental relay station in this pathway. To provide evidence for such an indirect tecto–tectal projection, we conducted anterograde and retrograde tracer injections into the left and/or right TeO. In the next paragraph, we first briefly describe some general findings regarding the afferents and efferents of the TeO, to show that our tectal injections were successful, and then turn to the results of the indirect tecto–tectal pathway. In the last section, we present results of our GABA and PV staining.

Afferent and efferent connections of TeO

Tectal injections revealed bilateral projections to the nucleus rotundus and ipsilateral efferents to the

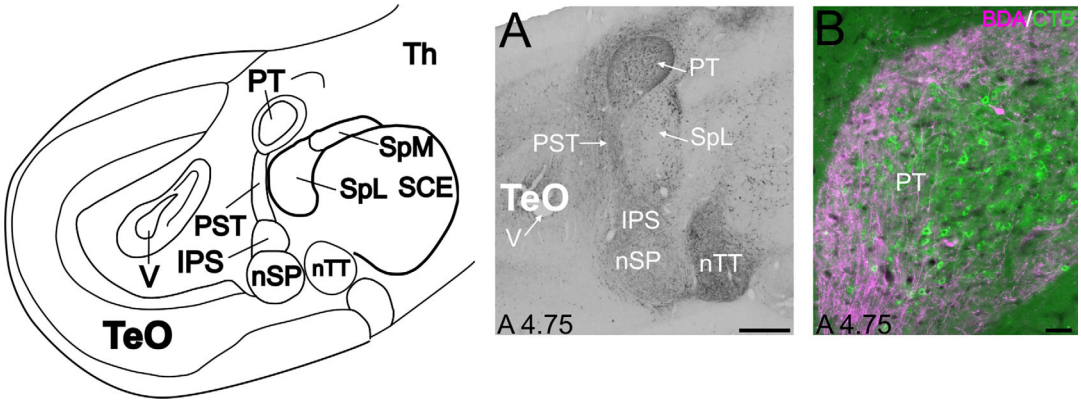

Figure 1. Mesencephalic afferents and efferents of the optic tectum. **A**: Schematic drawing of slice corresponding to pictures with higher magnification shown in B and C. **B**: Dense fiber innervation after CTB injection into the ipsilateral optic tectum was observed in the pretectal nucleus, subpretectal nucleus, nucleus of the tecto–thalamic tract, and interstitio–pretecto–subpretectal nucleus. Fibers were also stained in the pretecto–subpretectal tract. Retrogradely labeled neurons were observed bilaterally in the pretectal nucleus and ipsilaterally in the lateral spiriform nucleus. **C**: Pretectal nucleus in an animal injected with BDA (magenta) into the ipsilateral tectum and CTB (green) into the contralateral tectum, demonstrating a connection between the left and right tectum via the pretectal nucleus. Abbreviations: IPS, interstitio–pretecto–subpretectal nucleus; PT, pretectal nucleus; nSP, subpretectal nucleus; nTT, nucleus of the tecto–thalamic tract; PST, pretecto–subpretectal tract; SCE, stratum cellulare externum; SpL, lateral spiriform nucleus; SpM, medial spiriform nucleus; Th, thalamus; V, ventricle. Scale bar = 500 μm in B; 50 μm in C.

nucleus pretectalis (PT), nucleus subpretectalis, nucleus interstitio–pretecto–subpretectalis, and nucleus of the tecto–thalamic tract. This last structure is also called the brachium colliculi superioris by Hunt and Künzle (1976) or nucleus posteroventralis thalami by Mpodozis et al. (1996) (Fig. 1). Furthermore, a weak ipsilateral projection to the lateral spiriform nucleus (SpL) was observed.

The afferents to the TeO originated ipsilaterally in the SpL and bilaterally in the PT, the lateral reticular formation (FRL), and the lateral tegmentum (see below). Furthermore, the TeO was reciprocally connected with the ipsilateral parvocellular and magnocellular isthmic nuclei. A sparse reciprocal connection between the left and right TeO was also observed. Tecto–tectally projecting neurons were located predominantly in layers 13–15, with a few neurons scattered throughout layers 9–12.

In addition, the TeO received bilaterally telencephalic input from the arcopallium with a predominance from its intermediate subdivision. Ipsilateral telencephalic afferents were observed from the hyperpallium along the full anteroposterior extent of the hyperpallium apicale (HA; A 14.25–7.75; Karten and Hodos, 1967) and the ipsilateral temporo–parieto–occipital area (dorsolateral part between A 9.00 and 6.75) (Fig. 2).

The tecto-tegmento-tectal pathway

The tectonigral and nigrotectal connection

As outlined above, we expected a pathway from the TeO via the ipsilateral SNr to the contralateral TeO. Therefore, we first analyzed injections of anterograde tracers into the TeO to uncover the tecto–nigral component of the pathway. Figure 3 shows schematic drawings of frontal midbrain sections at the level of the substantia nigra (SN). Numerous labeled somata could be observed within and near the regions of the tracer injection. In the ipsilateral TeO, dense fiber staining was observed from layers 2 to 13, but smaller numbers of fibers were also present in layers 14 and 15. Moreover, large numbers of radially oriented processes were labeled within layers 3–5, presumably representing dendrites and axons of tectal neurons.

Many fibers left the TeO via the tecto–reticular tract. A large number of fibers were labeled within the ipsilateral lateral mesencephalic reticular formation (FRL). Some fibers reached the ipsilateral SN including both the dopaminergic pars compacta (SNc) and the SNr, indicating a weak tecto–nigral connection (Fig. 3).

In general, it is possible that the tecto–nigro–tectal pathway consists of fibers running from the TeO via the contralateral SNr to the other TeO. We therefore analyzed the tectal projections to the contralateral side. Crossing fibers took one of two possible pathways to cross the midline. Whereas a considerable number of fibers, especially at the rostral level around A 4.00, ran via the tectal and posterior commissures (CT/CP), other fibers crossed the midline through the tegmentum. Further caudally, although we still observed fibers in the CT, they were scarce. Several commissural fibers reached the contralateral TeO, particularly layer 15.

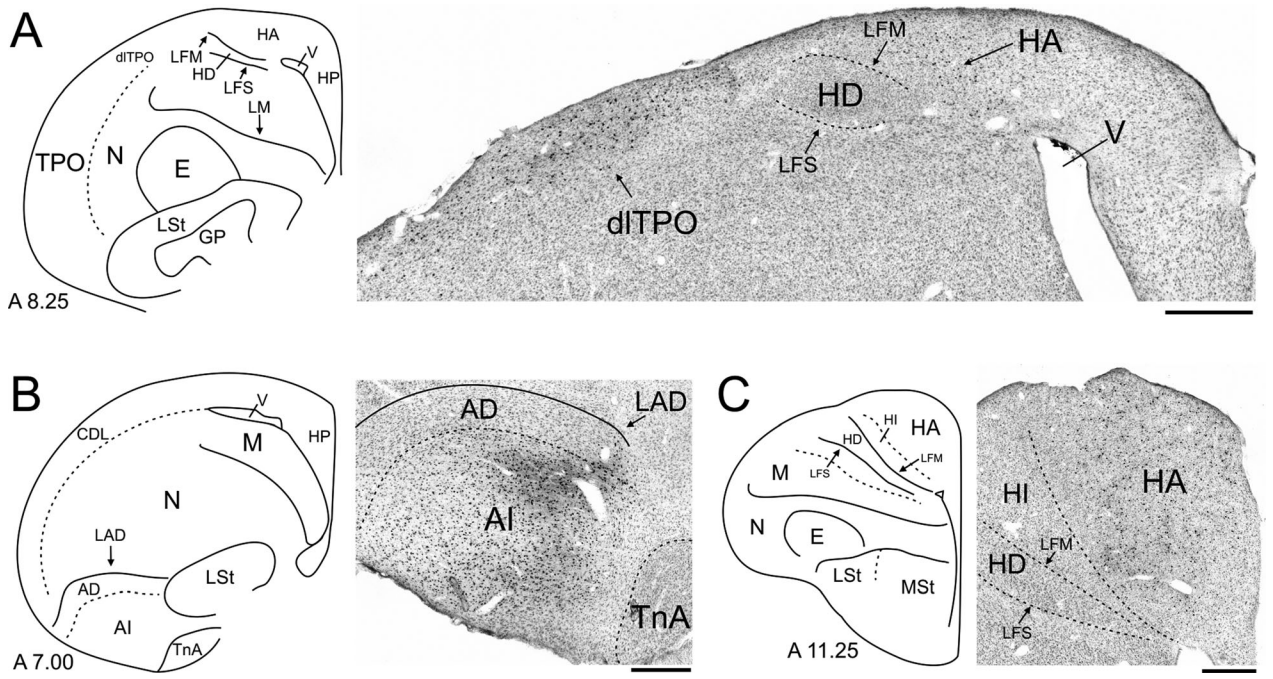

Figure 2. Telencephalic afferents to optic tectum. **A–C**: After injections of retrograde tracers into the optic tectum, many retrogadely labeled neurons were observed in the temporo–parieto–occipital area (A), intermediate arcopallium (B), and hyperpallium apicale (C). The animal shown in the figure received massive CTB injections into the left optic tectum. Projections from the hyperpallium and the temporo–parieto–occipital area were only ipsilateral, whereas the arcopallium projected weakly also to the contralateral optic tectum. Schematic drawings illustrate the labeled sections at lower magnification. Abbreviations: AD, dorsal acropallium; AI, intermediate arcopallium; CDL, area corticoidea dorsolateralis dlTPO, dorsolateral part of the temporo–parieto–occipital area; E, entopallium; HA, hyperpallium apicale; GP, globus pallidus; HD, hyperpallium dorsale; HI, intercalated hyperpallium; HP, hipoccampus; LAD, lamina arcopallialis dorsalis; LFM, lamina frontalis suprema; LFS, lamina frontalis superior; LM, lamina mesopallialis; LSt, lateral striatum; M, mesopallium; MSt, medial striatum; N, nidopallium; TnA, nucleus taeniae of the amygdala; TPO, temporo–parieto–occipital area; V, ventricle. Scale bar = 1,000 μm in A; 500 μm in B,C.

In the superficial layers, fibers were seen only sporadically.

The tegmental pathway crossed the midline just underneath the ventral oculomotor nucleus. After crossing, the majority of fibers remained within the brachium conjunctivum ascendens and descendens as well as within the medial longitudinal fascicle. Only few fibers were observed in the rest of the contralateral tegmentum (Fig. 3).

To investigate the nigrotectal component of our proposed pathway, we analyzed labeled neurons in the SNr after retrograde tracer injections into the TeO. TH staining was used to visualize the dopaminergic neurons of the SNc. This allowed better localization of the SNr, which lies dorsolaterally adjacent to the SNc in birds (Veenman and Reiner, 1994; Reiner et al., 2004). We observed a strong ipsilateral nigrotectal projection (Fig. 4A,C), whereas the contralateral projection was only very sparse (Fig. 4B,D). In sum, the TeO projects to the ipsilateral but not to the contralateral SNr, while the SNr projects back to the ipsilateral and only extremely sparsely to the contralateral TeO. Thus, a tecto–nigro–tectal projection in pigeons is not completely absent, but consists of only a very small group of neurons.

Nucleus of the lateral ponto–mesencephalic tegmentum

Although only a small number of contralateral nigrotectal cells were labeled after tectal injections, a remarkably large population of retrogradely labeled neurons could be detected within the contralateral lateral tegmentum (Fig. 5). These medium-sized multipolar neurons (Fig. 5E) were located ventromedially to the parvocellular and magnocellular isthmic nuclei in the region of descending tectopontine fibers (Figs. (5 and 6)). The rostrocaudal extent of this cell population was about 1.25 mm, from A 3.25 to A 2.00 (Fig. 6). Moreover, in contrast to other tectal afferents, this region almost exclusively projected to the contralateral TeO, with virtually no ipsilateral projections (Fig. 5C,D). Thus, this region could be a part of the proposed indirect tecto–tectal pathway. We further refer to this region as

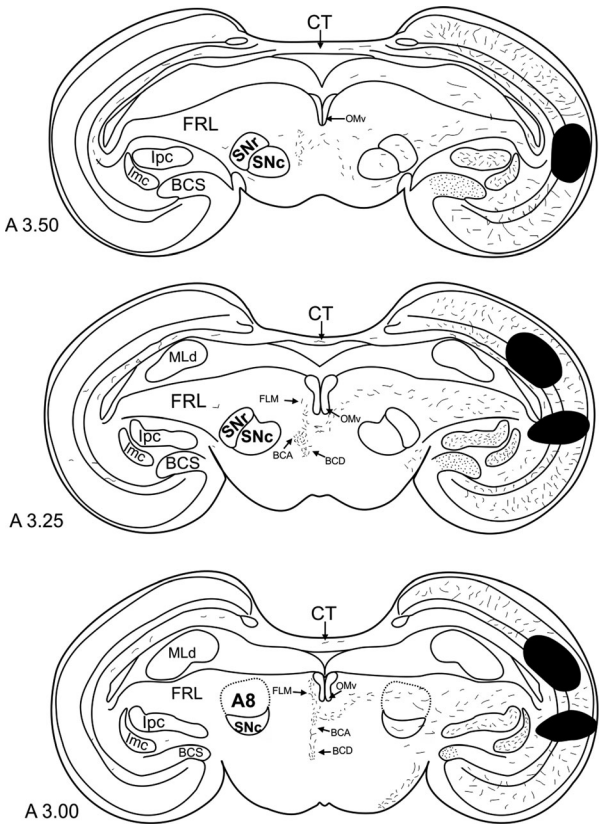

Figure 3. Schematic drawings of BDA-labeled fibers after BDA injections into the optic tectum. The drawings depict a case in which in total six injections (marked by black ellipsoids) along the anterior–posterior and ventral–dorsal axis were made into the right tectum. Note that fibers (represented by scattered lines) cross the midline via both the tectal commissura and the tegmentum; however, only the commissural pathway reaches the contralateral tectum. Some fibers are present in the ipsilateral but not in the contralateral substantia nigra. Abbreviations: BCA, brachium conjunctivum ascendens; BCD, brachium conjunctivum descendens; BCS, brachium colliculi superioris; CT, tectal commissure; FLM, medial longitudinal fascicle; FRL, lateral reticular formation; Imc, isthmic nucleus pars magnocellularis; Ipc, isthmic nucleus pars parvocellularis; MLd lateral mesencephalic nucleus pars dorsalis; OMv, ventral oculomotor nucleus; SNc, substantia nigra pars compacta; SNr substantia nigra pars reticulata.

the nucleus of the lateral ponto–mesencephalic tegmentum (nLPT).

To better characterize the neurochemical nature and exact location of the nLPT, we performed double immunostaining against CTB in combination with TH. This analysis revealed that the nLPT neurons with projections to the contralateral tectum were TH-negative and were juxtaposed ventrolaterally to the catecholaminergic neurons (Figs. (6 and 7)). The anterior tip of this tegmental nucleus was adjacent to the caudal SNc, the central part continued along the A8 region, and the most caudal portion was located ventrolaterally to the locus coeruleus (Fig. 6).

Ipsilateral tectal input to nLPT

To be part of the indirect tecto–tectal pathway, the nLPT needs to receive input from the ipsilateral TeO. Indeed, we observed fibers in this region after tracer injections into the TeO (Fig. 5C). To demonstrate a genuine disynaptic pathway between the tecta, we injected retrograde tracers (CTB or TDA) into one and the anterograde tracer BDA into the other TeO of the same animal (Fig. 8A). These tracings demonstrated fibers arising from the ipsilateral TeO in the vicinity of cells projecting to the contralateral TeO within the nLPT (Fig. 8B,C). In many cases it looked as if the fibers would encase the soma or its dendrites. Confocal microscopy analysis confirmed close appositions of ipsilateral tectal fibers and nLPT neurons (Figs. (9 and 10)), making it likely that tectal axons would contact the nLPT neurons and might form both axodendritic and axosomatic synapses (Fig. (9 and 10)).

Layer-specific origins and terminations

To confirm and further investigate the afferent and efferent connection between the nLPT and ipsilateral and the contralateral TeO, respectively, we made both anterograde and retrograde tracer injections into the nLPT (Fig. 11). After CTB injections into the nLPT (Fig. 11A), we observed retrogradely labeled neurons in layers 9–15 of the ipsilateral TeO (Fig. 11B–D). The majority of the neurons were located in layers 15 and 13. The labeled neurons were of different size, of oval, fusiform, or triangular shape, and had either horizontal or vertical orientations. In accordance with our tectal tracings, we also found anterogradely labeled fibers in the contralateral TeO after BDA injections into the nLPT (Fig. 11E,F–I). The majority of fibers with axon terminals were found in layers 5 and 10–13. Fibers also terminated in layers 6 and 14, although rarely. We observed only few if any fibers in layer 15; however, we did not see axon terminals in this layer.

Two ways to cross the midline

There are two possible ways that fibers from the nLPT could reach the contralateral TeO. We observed fibers crossing the midline via both the tectal commissure and the tegmentum. To accomplish a more detailed analysis of the axonal path, we switched to in vitro tracing, to achieve prominent labeling of axons along their whole trajectory (Fig. 12). Although we could observe fibers running toward the CT, especially in the more anterior in vitro injections (Fig. 12A,B), the results rather suggested that the vast majority of the fibers

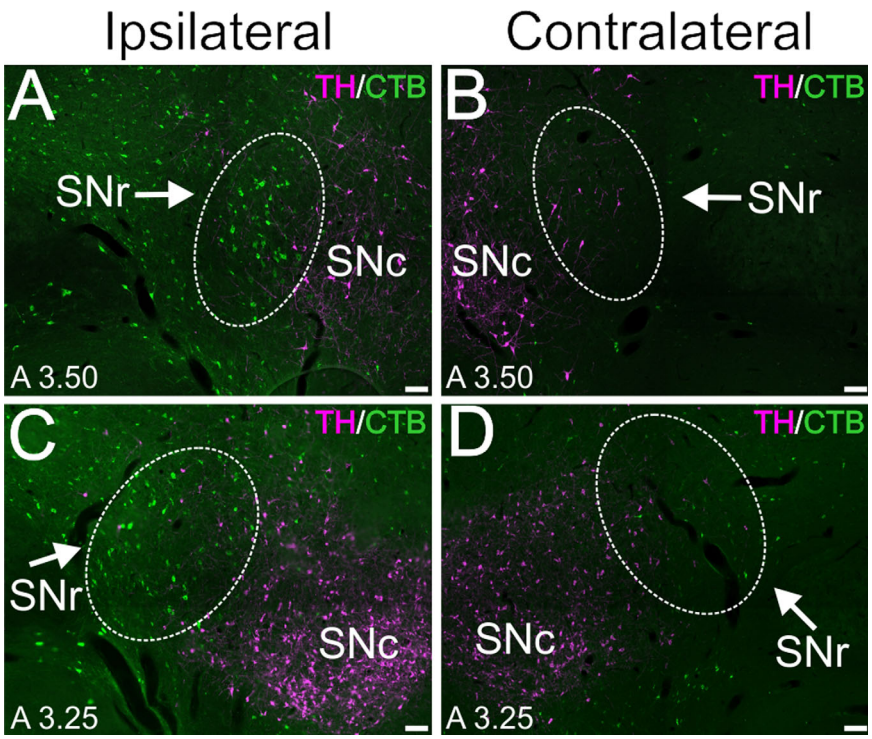

Figure 4. Tectopetal projections of the substantia nigra pars reticulata. **A,C**: Tectal injection of CTB revealed retrogradely labeled neurons (green) in the ipsilateral substantia nigra pars reticulata. **B,D**: Contralateral tectopetal projection of the substantia nigra pars reticulata was virtually not present. Neurons stained against tyrosine hydroxylase (magenta) represent the pars compacta of the substantia nigra. Abbreviations: SNc, substantia nigra pars compacta; SNr, substantia nigra pars reticulata. Scale bar = 100 μm in A–D.

cross via the tegmentum (Fig. 12A,C,D). We saw many fibers running from the nLPT toward the contralateral hemisphere crossing the midline just underneath the oculomotor nucleus and the medial longitudinal fascicle (Fig. 12D). However, we were not able to follow these fibers up to the tectal layers, because these axons had a curvature that ran perpendicular to the section, around the tectal ventricle (Fig. 12E).

nLPT projections are not topographically organized

Because many tectal connections display a topographic organization (Reiner et al., 1982a; Güntürkün and Remy, 1990; Wylie et al., 2009), we wondered whether the nLPT comprises some topographical subdivisions with respect to its tectopetal projections. Therefore, we made multiple unilateral injections of two retrograde tracers (TDA and CTB), with each tracer injected into different parts of the TeO. Injections were made into either the dorsal and ventral (Fig. 13A) or the anterior and posterior (Fig. 13B) TeO. All cases yielded an intermingled arrangement of retrogradely labeled neurons, indicating that the nLPT projected to the TeO in a nontopographical manner (Fig. 13C,D). We also observed some double-labeled neurons, possibly resulting from the overlap of the tracer spreads.

Further connectivity of nLPT

In addition to tectal labeling, CTB injections into the nLPT revealed retrogradely labeled neurons in the stratum cellulare externum (especially the posterior part), subthalamic nucleus, nucleus subrotundus, and ventrointermediate area of the thalamus. This last projection was extremely sparse. Some neurons were also scattered throughout the lateral and medial hypothalamus. In the telencephalon, we observed several neurons within the medial and lateral striatum, globus pallidus, ventral pallidum, and basal magnocellular nucleus. Large numbers of neurons were observed within the intermediate arcopallium (Fig. 14A–D).

BDA injections into the nLPT labeled axon terminals in pretectal structures and the nucleus rotundus, possibly as a result of tracer spread within the TeO, as the injection path had to penetrate the tectum. Besides that, several fibers were present within the medial and lateral hypothalamus. A considerable number of axon terminals were found in the posterior dorsal thalamus, within the dorsointermediate and posterior dorsolateral thalamic nuclei. A few terminals also reached the posterior dorsomedial thalamic nucleus. Several fibers

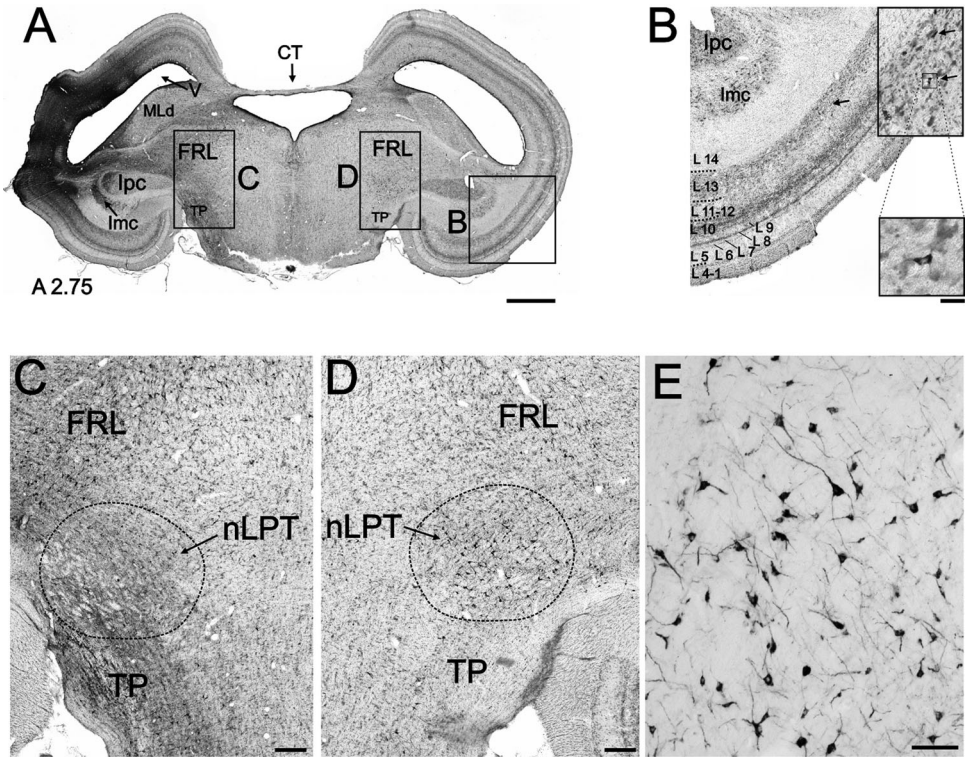

Figure 5. Contralateral tegmental afferents to the optic tectum. **A**: DAB-stained coronal section of the pigeon's midbrain counterstained with Nissl. CTB was injected into the left optic tectum. **B–D**: Magnifications of the selected regions. **B**: Direct tecto–tectal projections are sparse. Neurons were observed only rarely in the contralateral TeO. Arrow points to retrogradely labeled neuron in layer 13 magnified in the insets. **C**: The ipsilateral nLPT barely projects to the tectum. **D**: However, the nLPT projects densely to the contralateral tectum. **E**: Higher magnification of retrogradely labeled nLPT neurons projecting to the contralateral TeO without Nissl staining. Abbreviations: CT, tectal commissure; Imc, isthmic nucleus pars magnocellularis; Ipc, isthmic nucleus pars parvocellularis; MLd lateral mesencephalic nucleus pars dorsalis; TP, tecto–pontine tract; V, ventricle. Scale bar = 1,000 μm in A; 200 μm in B–D; 20 μm in the inset in B bottom and 50 μm in the upper inset in B and in E.

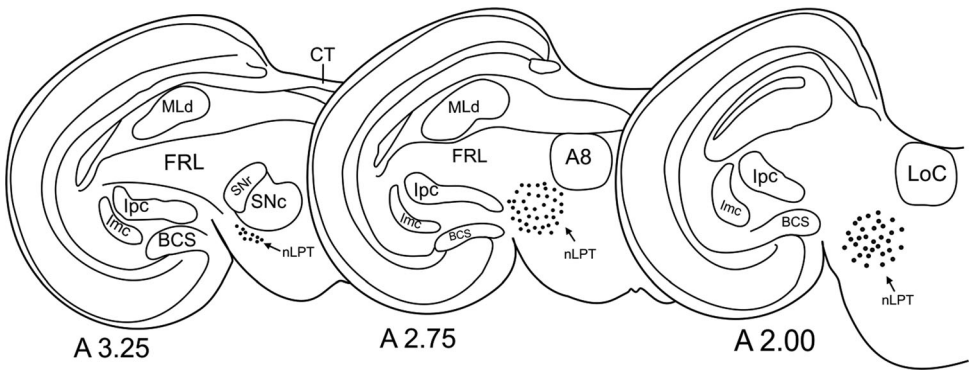

Figure 6. Location of the nLPT. The neurons were located ventrolaterally juxtaposed to the catecholaminergic regions of the substantia nigra pars compacta, region A8, and the locus coerlueus. The rostrocaudal extent of this nucleus was from A 3.25 to A 2.00. Abbreviations: BCS, brachium colliculi superioris; CT, tectal commissure; Imc, isthmic nucleus pars magnocellularis; Ipc, isthmic nucleus pars parvocellularis; LoC, locus coeruleus; MLd lateral mesencephalic nucleus pars dorsalis; nLPT, nucleus of the lateral ponto–mesencephalic tegmentum; SNc, substantia nigra pars compacta; SNr substantia nigra pars reticulata.

were also labeled in the ventrointermediate thalamic nucleus. Within the forebrain, we observed fibers travelling within the occipitomesencephalic tract and some fibers within the arcopallium. In addition, we observed a small number of axon terminals within the medial and lateral striatum and in the globus pallidus (Fig. 15).

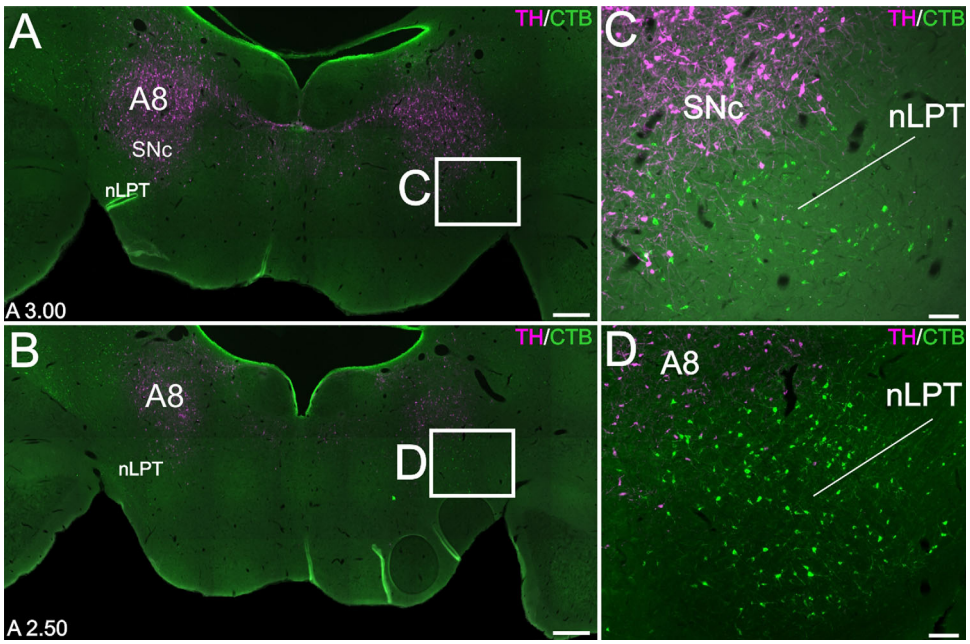

Figure 7. Topological relation between nLPT and catecholaminergic neurons. **A–D**: Neurons of the nLPT were located ventrolaterally along the catecholaminergic regions of the substantia nigra pars compacta and region A8. The rectangles in A and B represent the magnified region on the right (C,D). Magenta, tyrosine hydroxylase–positive neurons; green, CTB-labeled neurons projecting to the contralateral optic tectum. No double-labeled neurons were found. Abbreviations: SNc, substantia nigra pars compacta; nLPT, nucleus of the lateral ponto–mesencephalic tegmentum; Scale bar = 500 μm in A,C; 50 μm in B,D.

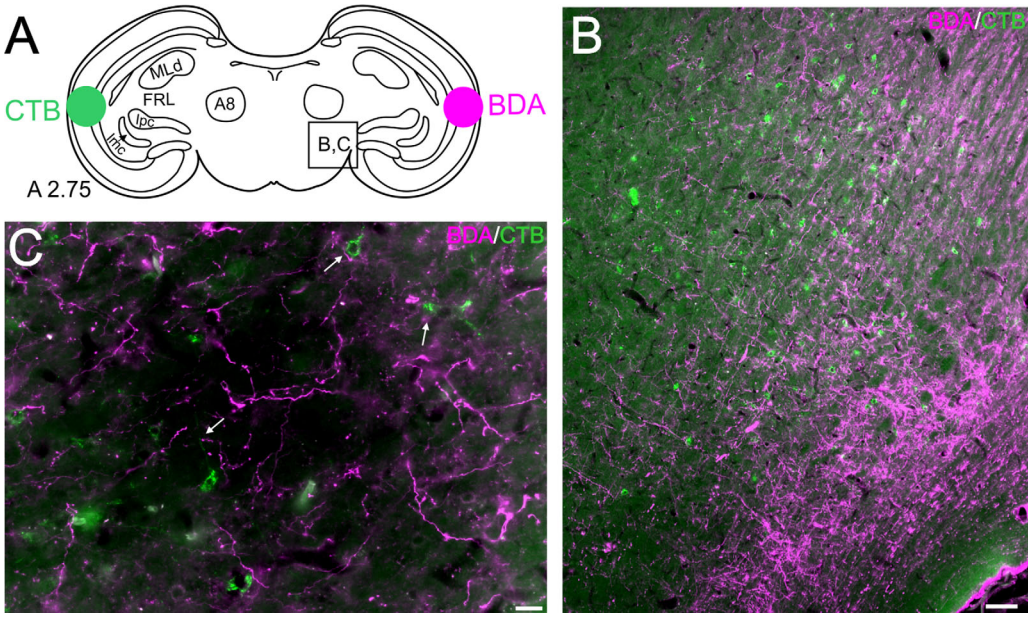

Figure 8. Bilateral antero- and retrograde tectal tracing. **A**: Rectangle in the schematic drawing shows the position of the nucleus magnified in B and C. **B,C**: Nucleus of the lateral ponto–mesencephalic tegmentum projects to the contralateral tectum and receives input from the ipsilateral tectum. The animal shown in the figure received a BDA injection into the right TeO and a CTB injection into the left TeO (C). White arrows point to examples of tectofugal fibers in the immediate vicinity of nLPT neurons, possibly indicating a synaptic contact between them. Scale bar = 50 μm in B; 20 μm in C.

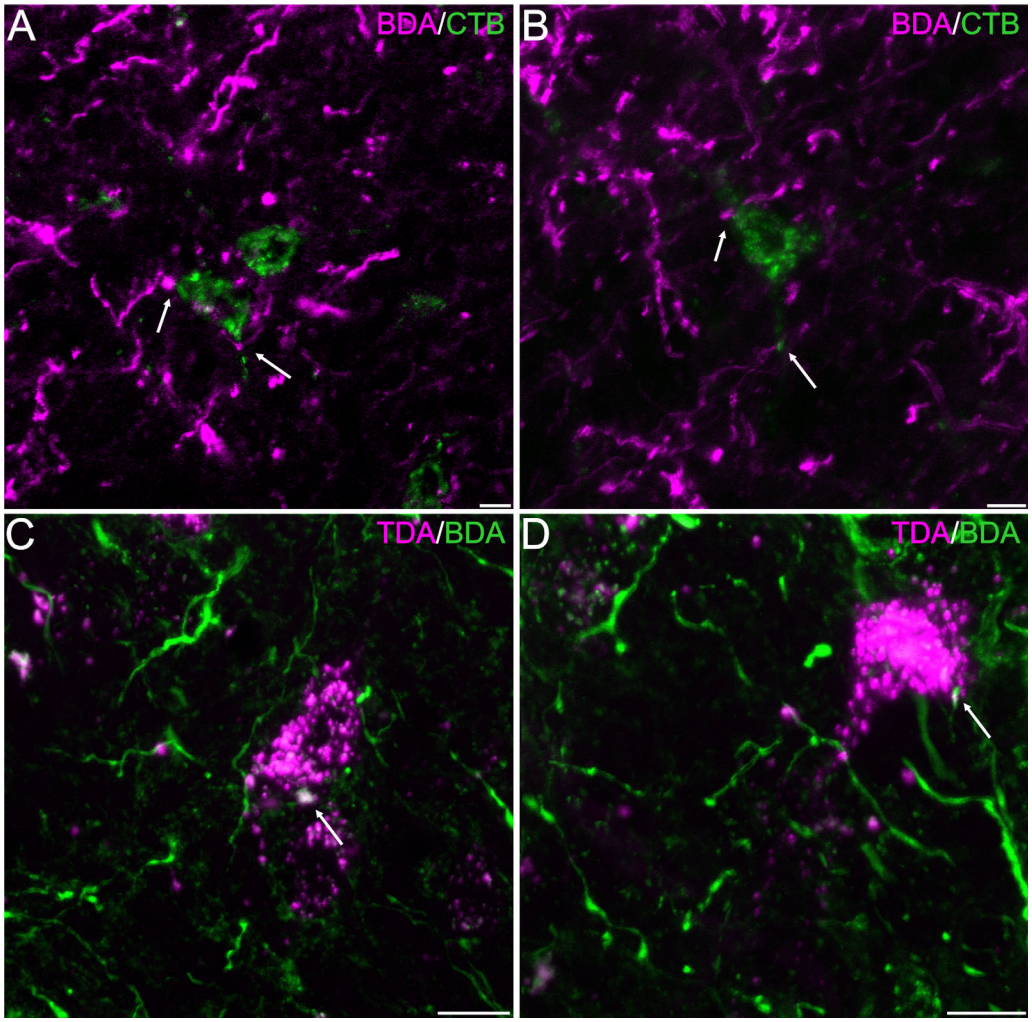

Figure 9. Input to nLPT from the ipsilateral optic tectum. Anterogradely labeled fibers originating in the ipsilateral tectum and retrogradely labeled cells in the nucleus of the lateral ponto–mesencephalic tegmentum (nLPT) projecting to the contralateral tectum. **A,B**: A case with a CTB injection into the left optic tectum and a BDA injection into the right optic tectum. **C,D**: A case with TDA injection into the right and BDA into the left tectum stained magenta and green, respectively. In all pictures, it is obvious that fibers reach close proximity to the neurons (white arrows). The apposition of fibers and neurons and the colocalization of magenta and green signal (white arrows in C and D) make synaptic contacts likely. The slices were analyzed with a confocal microscope. Scale bar = 10 μm in A–D.

Unfortunately, due to the close proximity of the nLPT to the SNc and A8, we did not succeed in injecting tracer into the nLPT only, without any spread into these neighboring structures. To ensure that the connectivity with striatal and pallidal areas and subthalamic and some thalamic nuclei did not arise due to possible spread of tracer into the adjacent SNc and A8 (Kitt and Brauth, 1981; Kitt and Brauth, 1986; Anderson and Reiner, 1991; Medina et al., 1997; Medina and Reiner, 1997), we analyzed cases with "near-miss" injections, with spread into the nLPT but without spread into other critical regions connected with basal ganglia (Fig. 14D–G). In these cases, we observed similar, although much weaker, connectivity patterns as in the nLPT injections. Similar to the nLPT, axon terminals were found in the ventrointermediate area of the thalamus and posterior dorsolateral thalamus, and several labeled neurons were found in the nucleus subrotundus. In cases with a small spread into the nLPT (Fig. 14E,F), only one retrogradely labeled neuron was found in the subthalamic nucleus and one in the globus pallidus, with no neurons in the striatum, whereas in a case with much larger spread into the nLPT (Fig. 14G), many retrogradely neurons in the globus pallidus and several in the lateral striatum could be found.

Results of GABA staining

Because the left and right TeO were shown to exert inhibitory interactions (Robert and Cuénod, 1969a,b; Keysers et al., 2000), we assumed that the projections

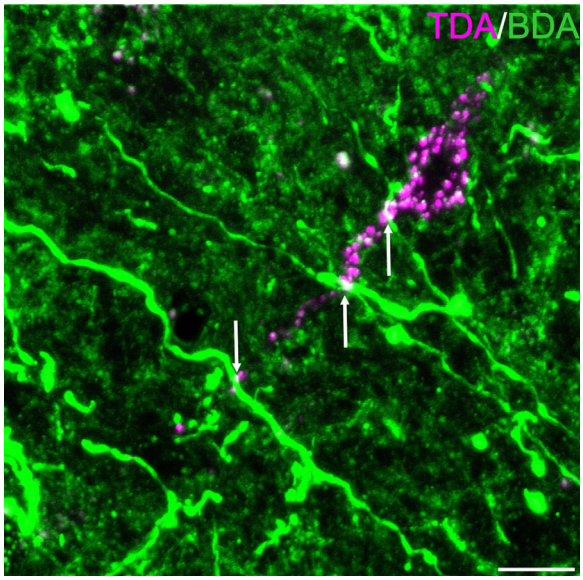

Figure 10. Putative axo–dendritic synapses on nLPT neurons. The picture shows a retrogradely labeled neuron in the left nLPT after injection of TDA into the right tectum and anterogradely labeled fibers after BDA injection into the left tectum. White arrows show colocalization of magenta (dendrite) and green (fibers) signal, which might indicate axo–dendritic synapses. Scale bar = 10 μm.

of a relay station constituting the indirect tecto–tectal pathway are GABAergic. To characterize the neurochemical nature of the tectopetal projections, we combined retrograde tectal tracing with GABA immunohistochemistry. Because the interaction between the left and right TeO is modulated top-down by pallial regions (Valencia-Alfonso et al., 2009), we were also interested in the neurochemical nature of this input. Therefore we also looked at the CTB-labeled telencephalic afferents combined with GABA staining.

nLPT

To test whether the nLPT can directly execute inhibitory effects on the contralateral TeO, we examined whether the nLPT neurons projecting to the contralateral TeO expressed the inhibitory neurotransmitter GABA. Confocal analysis of this double staining verified that many neurons in the nLPT projecting to the contralateral TeO were GABAergic (Figs. (16 and 17)). However, considerable numbers of neurons remained only either GABA or CTB/TDA labeled.

Telencephalon

CTB/GABA double staining demonstrated that neurons in the arcopallium (Fig. 18A), hyperpallium (Fig. 18B), and temporo–parieto–occipital area (Fig. 18C) that project to the TeO are very likely not GABAergic (Fig. 18). Although GABAergic neurons were scattered throughout these regions, they were distinct from the CTB-labeled neurons.

SNr

Although our tracing results showed that the SNr is not involved in tecto–tectal communication, we nevertheless observed projections of the SNr to the ipsilateral TeO. In mammals, the projection of the SNr to the SC is exclusively GABAergic (Araki et al., 1984). In contrast to the mammalian pattern, the results of our CTB/GABA double labeling in the SNr showed that GABAergic neurons and tectally projecting SNr cells were rather distinct populations (Fig. 19AB). The GABAergic neurons of the SNr were shown to coexpress the calcium-binding protein PV (Reiner and Anderson, 1993). Therefore, we chose PV to confirm the negative results. Similarly, PV-positive neurons and tectally projecting neurons formed virtually distinct populations (Fig. 19D–F). A subsequent PV/GABA double labeling revealed that virtually all PV-positive neurons in the SNr were GABAergic, although there were still some GABAergic neurons that were PV negative (Fig. 19C). Thus, our GABA and PV immunohistochemistry demonstrated that, with the exception of very few cells, the projection of the SNr to the TeO in birds is not GABAergic.

SpL

The data above showed that the SNr is unlikely to exert GABAergic inhibition onto the TeO. We therefore wondered whether the missing ipsilateral inhibitory input from the SNr is compensated by another system in birds. Because the connectivity of the SpL is similar to that of the SNr (Reiner et al., 2005; Kuenzel et al., 2011) and because the SpL also contains GABAergic neurons (Veenman and Reiner, 1994), we examined whether the projection of the SpL to the ipsilateral TeO arises from these GABAergic neurons. The results demonstrated that the majority of SpL neurons with projections to the TeO were indeed GABA positive (Fig. 20A). Similar to the SNr, PV- and GABA-positive neurons were colocalized in the SpL (Reiner and Anderson, 1993). We again performed PV staining to confirm the results of the GABA immunohistochemistry. Many tectally projecting neurons were PV positive, although a number of neurons were not double labeled (Fig. 20C). Similar to the SNr, virtually all PV neurons were GABAergic, but a few GABAergic neurons did not coexpress PV (Fig. 20B,D).

DISCUSSION

In this study, we conducted an anatomical analysis of the systems involved in tecto–tegmento–tectal communication in pigeons and report three main results.

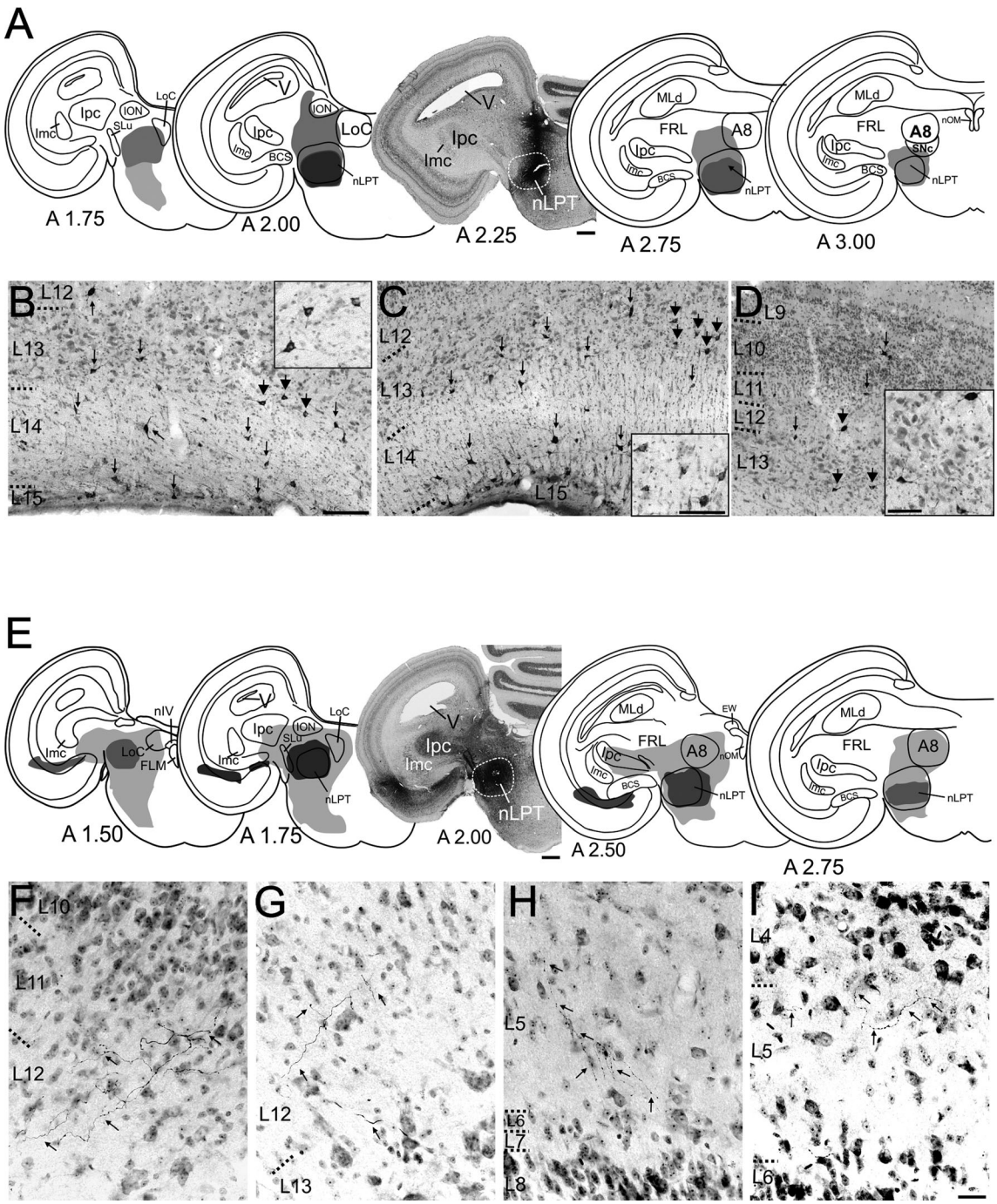

Figure 11. Laminar origins and terminations of tectal afferents and efferents of the nLPT. **A,E**: The figure shows one CTB (A) and one BDA (E) injection into the nLPT. The spread of the tracer is drawn on the schematic drawings of transversal sections anterior (right) and posterior (left) to the injection site shown in the photographs. The intensity of the color indicates the intensity of tracer spread. The BDA injection into the nLPT (E) was performed laterally via the tectum, whereas the CTB injections into the nLPT (A) was done with a dorsal approach. **B–D**: Retrogradely labeled neurons in the ipsilateral tectum after CTB injection shown in A into the nLPT. The neurons were located in layers 9–15, with the majority in layers 15–13. The arrows with larger heads point to neurons shown in insets. **F–I**: BDA-labeled fibers (black arrows) in the contralateral tectum after the injection into the nLPT shown in E. The fibers terminated mainly in layers 10–13 and 5 and 6. All sections are counterstained with Nissl. Abbreviations: BCS, brachium colliculi superioris; EW, Edinger–Westphal nucleus; FLM, medial longitudinal fascicle; FRL, lateral reticula formation; Imc, isthmic nucleus pars magnocellularis; ION, isthmo-optic nucleus; Ipc, isthmic nucleus pars parvocellularis; LoC, locus coerlueus; MLd lateral mesencephalic nucleus pars dorsalis; nOM, nucleus nervi oculomotorii; nLPT, nucleus of the lateral ponto–mesencephalic tegmentum; nIV, nucleus nervi trochlearis; SLu, nucleus semilunaris; SNc, substantia nigra pars compacta; V, ventricle. Scale bar = 1,000 μm in A,E; 100 μm in B–D for low magnification images; 50 μm in the insets B–D; 20 μm in I (applies to F–I).

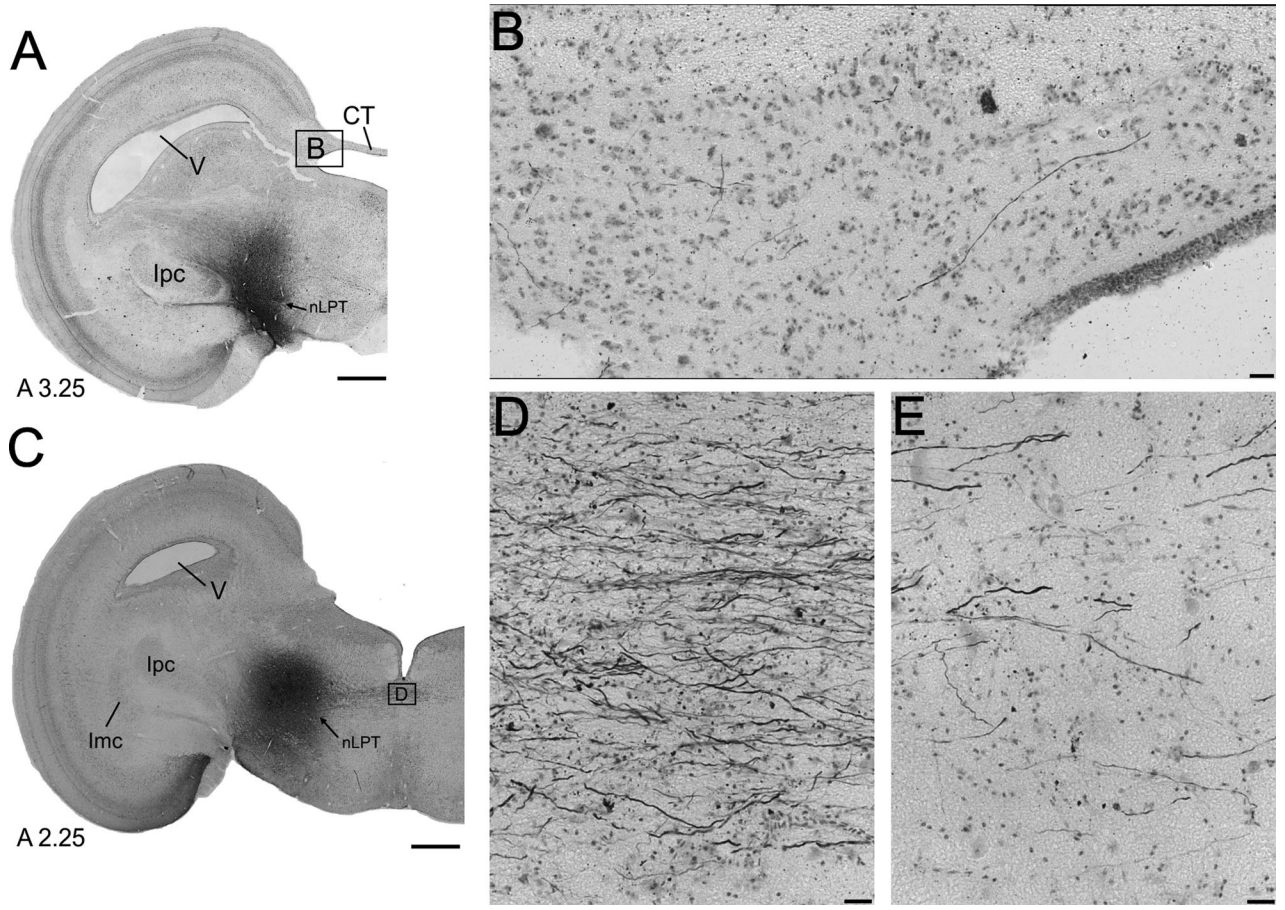

Figure 12. Axons of the contralaterally projecting nLPT neurons cross predominantly via the tegmentum. **A**: Biocytin injection into the rostral nLPT revealed fibers running from the nLPT toward the tectal commissura as well as toward the ventral tegmentum. **B**: Fibers running toward the tectal commissura (magnification of the region marked with rectangle in A). **C**: BDA injections into the caudal nLPT revealed that the majority of fibers originating in the nLPT cross the midline via the tegmentum rather than via the commissura. **D**: BDA-labeled fibers crossing the midline (rectangle in C). **E**: Fibers gradually disappear in the contralateral tegmentum, as they appear to run perpendicularly to their ipsilateral plane to overcome the tectal ventricle. Sections are counterstained with Nissl. Abbreviations: Imc, isthmic nucleus pars magnocellularis; Ipc, isthmic nucleus pars parvocellularis; nLPT, nucleus of the lateral ponto–mesencephalic tegmentum; V, ventricle. Scale bar = 1,000 μm in A,B; 50 μm in C; 20 μm in D,E.

First, we discovered a novel tegmental region in the brainstem of the pigeon (nucleus of the lateral ponto–mesencephalic tegmentum; nLTP) that receives input from the ipsilateral TeO and provides GABAergic output to the contralateral TeO. Thus, this system possibly constitutes the main anatomical substrate for inhibitory tecto–tectal interactions (Fig. 21). Second, our data revealed that the SNr does not project to the contralateral TeO and therefore possibly does not participate in tecto–tectal interactions. Third, the virtually exclusive ipsilateral projection from the SNr to the TeO is for the most part not GABAergic in pigeons. All these characteristics differ from the mammalian tectopetal projection pattern. We therefore speculate that the emergence of the tectopetal projection originating in the GABAergic neurons of the SpL rendered the inhibitory nigrotectal pathway obsolete during avian evolution. Furthermore, the ipsilaterality of tectopetal systems possibly promoted the appearance of a novel tegmental region, the nLPT, to support interhemispheric communication. We first briefly discuss the organization of the avian substantia nigra and then speculate about the emergence and nature of the nLPT and its putative function.

Organization of the avian substantia nigra

The avian SNr is homologous to the mammalian SNr (Reiner et al., 2004). It receives input from GABAergic striatal neurons that cocontain substance P (SP) (Reiner et al., 1983; Hall et al., 1984; Anderson and Reiner, 1991). Further afferents arise from the GABAergic pallidal neurons, which themselves receive input from the

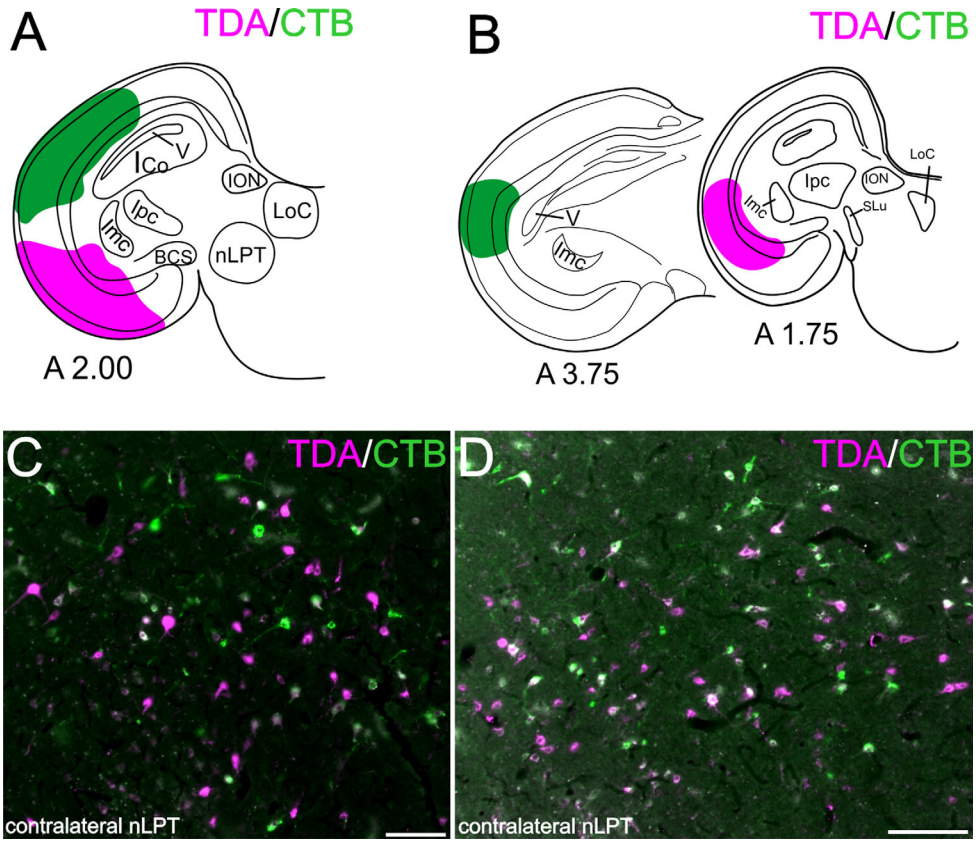

Figure 13. Nontopography of the nLPT. **A**: Injections into the dorsal and ventral tectum revealed an intermingled picture of retrogradely labeled neurons in the contralateral nLPT (**C**). Similarly, anterior (**B**, left) and posterior (**B**, right) injection in the same animal revealed a comparable picture (**D**). These results demonstrate that neurons projecting to different parts of the optic tectum are intermingled in the nLPT. Scale bar = 100 μm in B,D.

enkephalinergic striatal neurons (Hall et al., 1984; Medina and Reiner, 1997; Medina et al., 1999). Excitatory input reaches the SNr from glutamatergic neurons of the subthalamic nucleus (STN) (Jiao et al., 2000). The SNr projects to the ventrointermediate area of the thalamus (VIA), a putative homologue of the mammalian motor thalamus (Medina et al., 1997), and to the TeO (Hunt and Brecha, 1984). It was assumed that the SNr–TeO projection originates in the GABAergic neurons of the SNr (Hunt and Brecha, 1984; Veenman and Reiner, 1994; Veenman, 1997; Medina et al., 1999). However, this is based on separate tracing (Hunt and Brecha, 1984) and GABA immunohistochemical experiments (Veenman and Reiner, 1994). To the best of our knowledge, a double-labeling study for this subject has not yet been published in birds. Our tectal tracing combined with the GABA immunohistochemistry could now demonstrate that the GABAergic and the tectum-projecting neurons of the SNr represent distinct populations. In both mammals and birds, GABAergic SNr neurons also express PV (Gerfen et al., 1985; Reiner and Anderson, 1993; McRitchie et al., 1996). Our immunostaining verified the colocalization of PV and GABA in the SNr but also demonstrated that only very few PV-immunoreactive neurons in the SNr project to the TeO.

The indirect tecto–tectal pathway

SNr—a relay station in the indirect tecto–tectal connection?

Our retrograde tracer injections into the TeO revealed that tectal neurons directly projecting to the contralateral TeO are sparse. However, the thickness of the commissura tectalis (Ehrlich and Saleh, 1982), which connects the left and the right TeO (Voneida and Mello, 1975; Hunt and Künzle, 1976), suggests that a much higher number of tectal neurons are involved in tecto–tectal communication. Previous electrophysiological studies showed that the avian tecta can inhibit each other via mono- and polysynaptic pathways (Robert and Cuénod, 1969a,b; Hardy et al., 1984; Keysers et al., 2000). Based on the mammalian literature (Gerfen et al., 1982; Bickford and Hall, 1992; Liu and Basso, 2008), we hypothesized that the SNr represents the relay station of the tecto–tectal connection that compensates for the paucity of direct tecto–tectal projections.

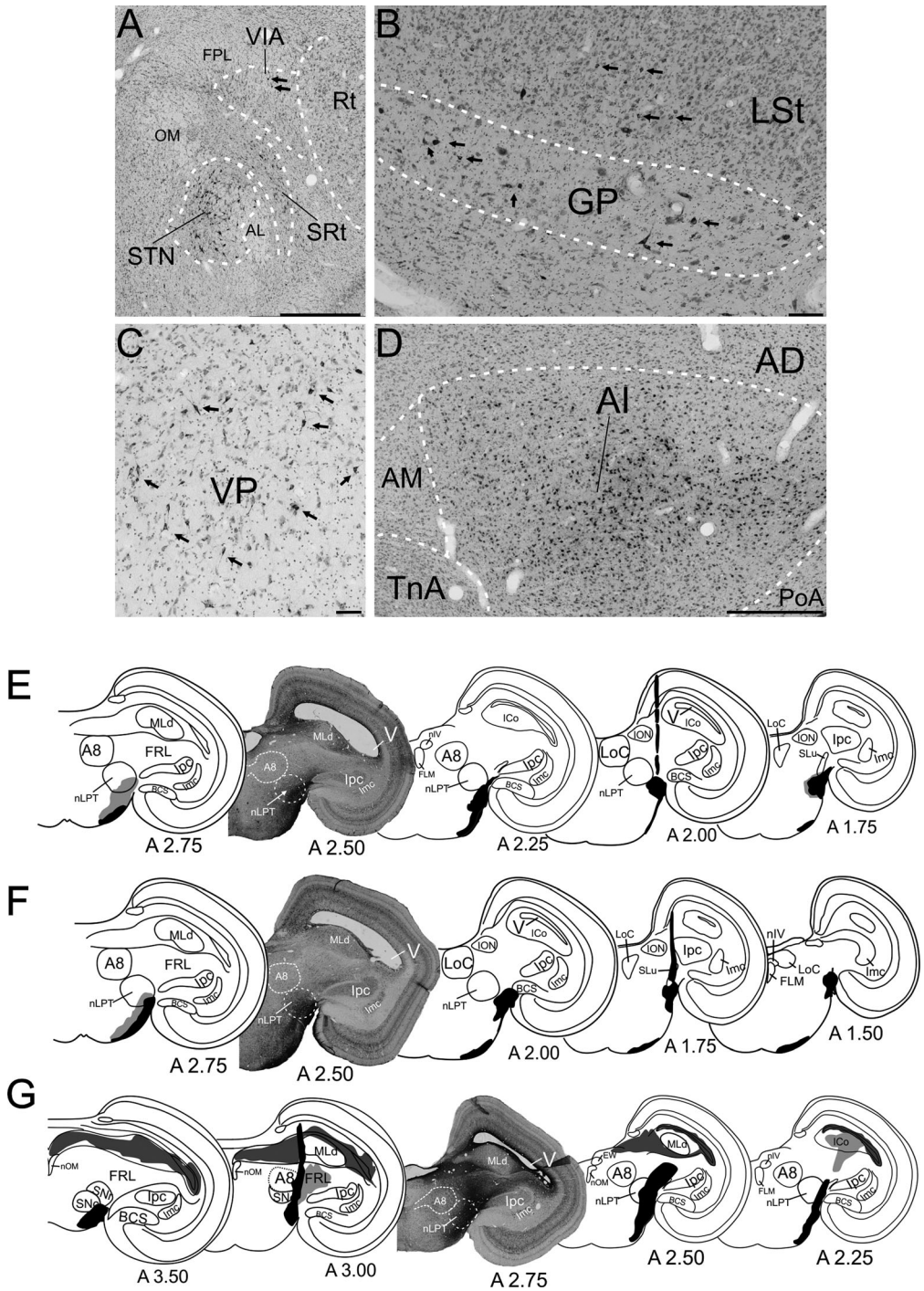

Figure 14. Afferents of the nLPT. **A**: Retrogradely labeled neurons after CTB injections into the nLPT in the subthalamic nucleus, subrotundal nucleus, and ventrointermediate nucleus of the thalamus. **B,C**: Retrogradely labeled neurons were also observed in striatal and pallidal regions and in the arcopallium. Arrows point to examples of retrogradely labeled cells. Sections are counterstained with Nissl. The injection site for the case presented is depicted in Figure 11A. **E–G**: Illustration of "near-miss" injections into the nLPT with spread into the nLPT but not into adjacent basal ganglia-related structures. Abbreviations: AI, intermediate arcopallium; AL, ansa lenticularis; BCS, brachium colliculi superioris; EW, Edinger–Westphal nucleus ; FLM, medial longitudinal fascicle; FPL, lateral forebrain bundle; FRL, lateral reticula formation; GP, globus pallidus; Imc, isthmic nucleus pars magnocellularis; ION, isthmo-optic nucleus; Ipc, isthmic nucleus pars parvocellularis; LoC, locus coerlueus; LSt, lateral striatum; MLd lateral mesencephalic nucleus pars dorsalis; nOM, nucleus nervi oculomotorii; nLPT, nucleus of the lateral ponto-mesencephalic tegmentum; nIV, nucleus nervi trochlearis; OM, occipito–mesencephalic tract; Rt, nucleus rotundus of the thalamus; SLu, nucleus semilunaris; SNc, substantia nigra pars compacta; SRt, subrotundal nucleus; STN, subthalamic nucleus; TnA, nucleus taniae of the amygdala; V, ventricle; VIA, ventrointermediate nucleus of the thalamus; VP, ventral pallidum. Scale bar = 500 μm in A,D; 100 μm in B,C.

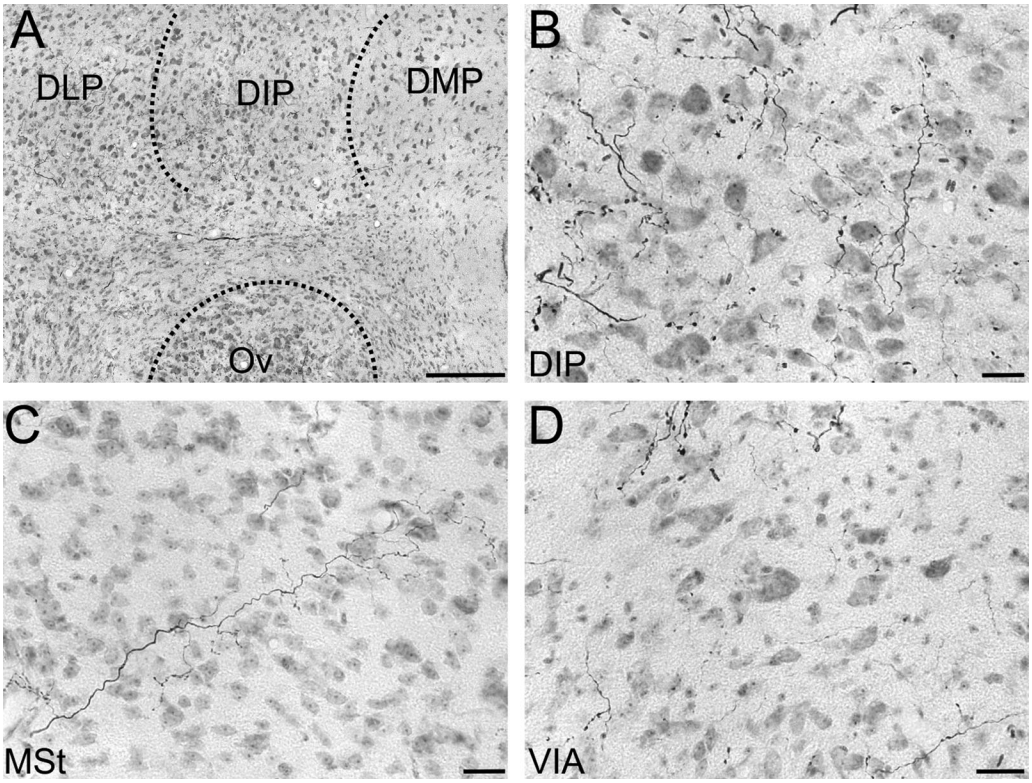

Figure 15. Efferents of the nLPT. Axonal terminations after BDA injections into the nLPT in the posterior dorsal thalamus (**A,B**), medial striatum (**C**), and ventrointermediate thalamic nucleus (**D**). Sections are counterstained with Nissl. The injection site for the case presented is depicted in Figure 11E. Abbreviations: DIP, dorsointermediate posterior thalamic nucleus; DLP, dorsolateral posterior thalamic nucleus; DMP, dorsomedial posterior thalamic nucleus; MSt, medial striatum; VIA, ventrointermediate thalamic nucleus. Scale bar = 200 μm in A; 20 μm in B–D.

The mammalian SNr gives rise to bilateral collicular projections of which the contralateral one is weaker (Rinvik et al., 1976; Grofová et al., 1978; Beckstead and Frankfurter, 1982; Gerfen et al., 1982; May and Hall, 1986; Harting et al., 1988; Bickford and Hall, 1992; Deniau and Chevalier, 1992). In contrast to this pattern, our experiments showed that the avian SNr projects to the ipsilateral but not (or only very weakly) to the contralateral TeO. Thus, the SNr cannot constitute a major relay station in the indirect tecto–tectal system. It is unlikely that the missing contralateral projection of the SNr is an artifact of our tracing. We performed massive injections into all parts of the TeO and observed both ipsi- and contralateral labeling, as reported in previous studies of tectal connectivity (Voneida and Mello, 1975; Hunt and Künzle, 1976; Reiner et al., 1982a,b; Rodman and Karten, 1995; Gamlin et al., 1996; Hellman and Güntürkün, 2001; Luksch, 2003; Hellman et al., 2004). In addition, we observed a tectal input to the SpL, which has not been reported before, possibly due to its sparseness (Hunt and Künzle, 1976; Reiner et al., 1982a).

The nucleus of the lateral ponto–mesencephalic tegmentum (nLPT) and the indirect tecto–tectal pathway

Posterior to the SNr and ventrolaterally to the catecholaminergic cell groups, we discovered a region in the lateral tegmentum that is very likely involved in disynaptic tecto–tectal inhibition. We named this region the nucleus of the lateral ponto–mesencephalic tegmentum (nLPT). The nLPT is TH negative and consists of GABAergic neurons projecting to the contralateral TeO (Fig. 21). We demonstrated that the nLPT receives monosynaptic input from the ipsilateral TeO originating mainly in layers 13–15 and projects to the contralateral TeO, predominantly to layers 5 and 10–13. Interestingly, these termination layers overlap with those of the PT and SpL, which end in layer 5b and in layers 8–13, respectively (Gamlin et al., 1996; Reiner et al., 1982a,b). Thus, the nLPT might interact with these projections and could influence descending motor and ascending visual pathways (Reiner and Karten, 1982; Hellmann et al., 2004). Because our CTB injections into

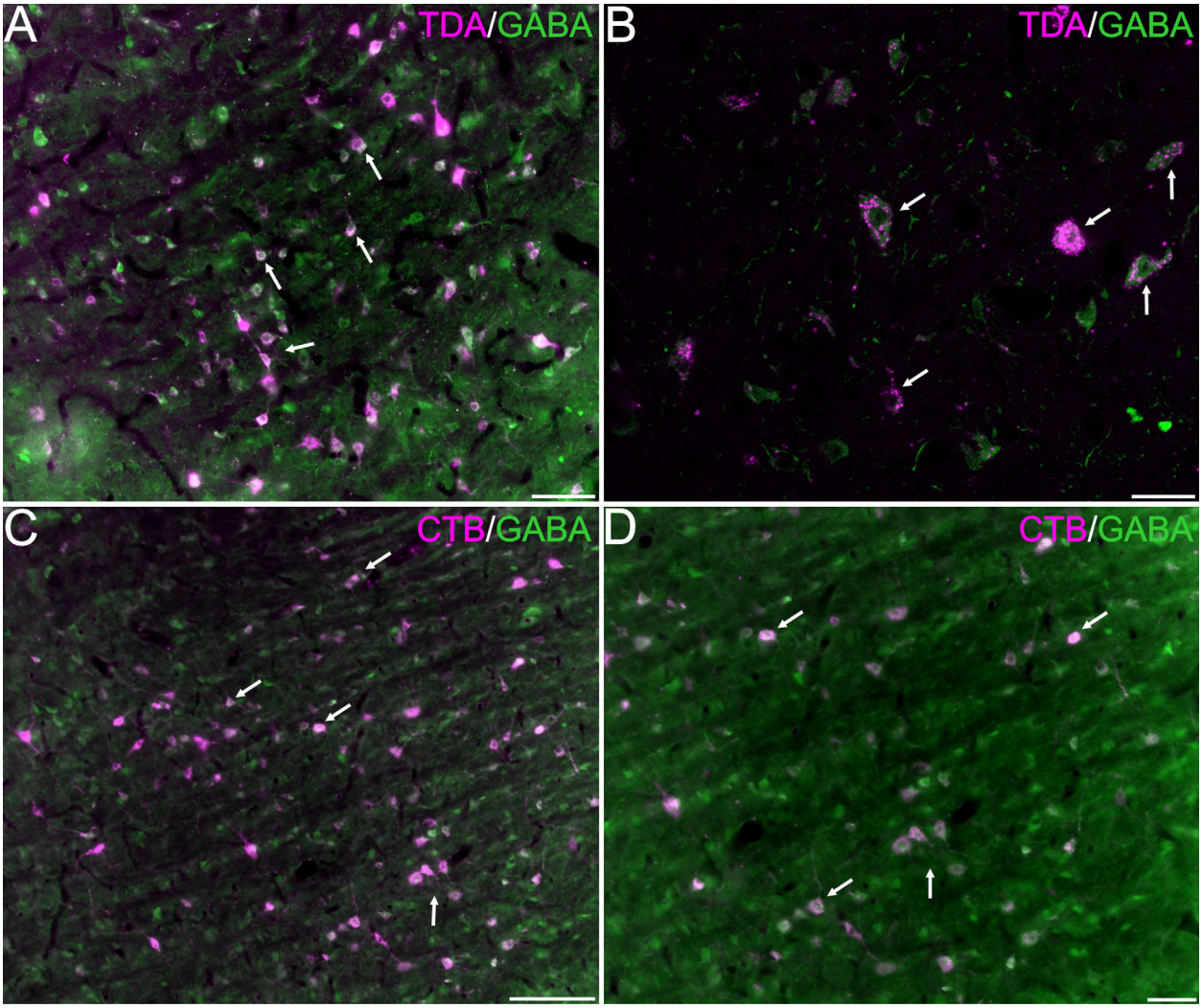

Figure 16. The majority of nLPT neurons are GABAergic. Double labeling of tectally projecting neurons (magenta) in the nLPT and GABA (green). **A**: The right nLPT after TDA injection into the left tectum. **B**: Magnification of some cells in A with a confocal microscope. **C**: The right nLPT after CTB injection into the left optic tectum. **D**: Magnification of some cells in C. A large percentage of CTB-positive neurons was double-labeled. The white arrows point out some examples of double-labeled neurons. There were also many neurons that were either GABAergic or tectally projecting. Scale bar = 50 μm A,D; 20 μm in B; 100 μm in C.

the nLPT were given dorsally, we cannot exclude the possibility that some retrogradely neurons in layer 10 represent isthmo-tectal neurons labeled due to tracer spread in the isthmo-optic nucleus (Woodson et al., 1991). In addition, because several tectofugal fibers run via the nLPT, some of the observed retrogradely labeled neurons may represent neurons projecting to other brainstem regions (Reiner and Karten, 1982; Hellmann et al., 2004). These neurons, however, may still collateralize in the nLPT. Furthermore, our results show that the nLPT does not comprise topographical subdivisions with respect to its output. Instead, its organization resembles the mosaic-like arrangement that is typical of tectal layer 13, where neurons with ascending projections to different parts of the nucleus rotundus, or with descending projections to different brainstem nuclei, are intermixed (Hellmann and Güntürkün, 1997; Marín et al., 2003; Hellmann et al., 2004).

Because the most anterior tip of the nLPT reached the level A 3.25 (Figs. 4D, green neurons at the bottom, and 6), and GABAergic neurons are also present in the anterior tip of the nLPT (Veenman and Reiner, 1994), one can easily get the impression that the nLPT and SNr are confluent. Thus, although the SNr and nLPT are certainly not overlapping, they might form one continuous structure with one rostral (SNr) and one caudal (nLPT) extension.

Phylogenetic considerations

The discovery of this novel region in the avian tegmentum sparks several questions. First, to which

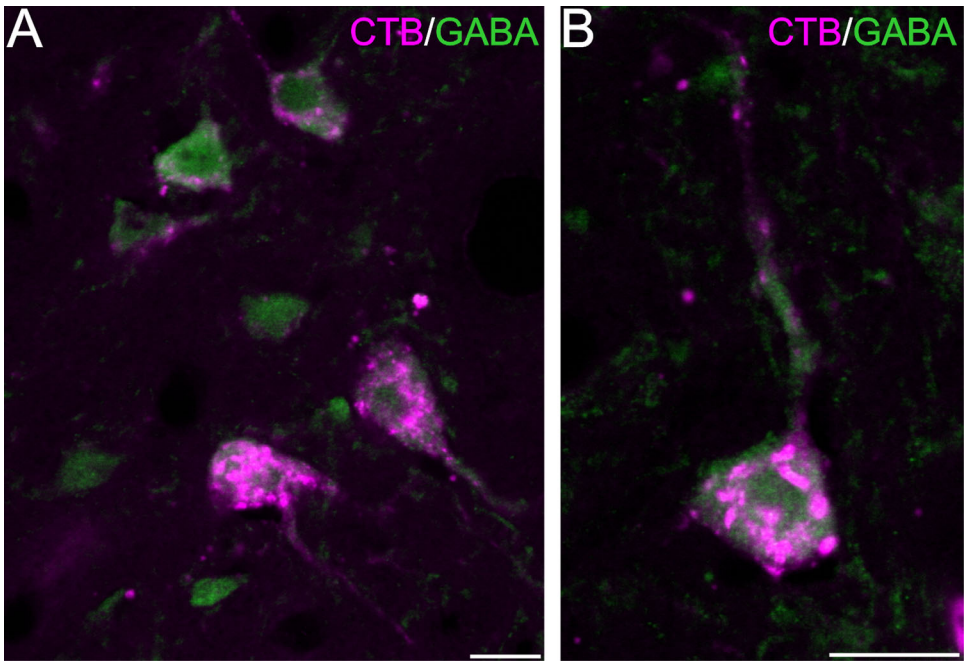

Figure 17. Neurons in the nLPT are GABAergic. Neurons in the nLPT projecting to the contralateral optic tectum express GABA. **A,B**: CTB-labeled neurons (magenta) in the nLPT double-stained with GABA (green). The photos were taken with a confocal microscope. Green, GABA; magenta, CTB; Scale bar = 10 μm in A,B.

system does the nLPT belong? Second, is this nucleus an apomorphic feature of the avian taxon? Our results indicate that the nLPT is associated with the basal ganglia, although we cannot exclude the possibility that at least part of the observed connectivity with striatal and pallidal areas and subthalamic and thalamic nuclei was due to the spread into the adjacent SNc and A8 (Kitt and Brauth, 1981, 1986; Anderson and Reiner, 1991; Medina et al., 1997; Medina and Reiner, 1997). The GABAergic nature of the nLPT and its striatal, pallidal, and subthalamic input and thalamic output indicates that the nLPT could be a caudal extension of the SNr.

We were surprised to see that the ipsilateral projection of the SNr to the TeO in birds is not GABAergic. Because GABAergic SNr–TeO projection seems to be a conserved vertebrate feature (Araki et al., 1984; Reiner et al., 1998; Stephenson-Jones et al., 2012), our data might suggest that the GABAergic nature of this projection was lost in the avian taxon (at least in Columbiformes). In amphibians, reptiles, and birds, a pathway running via the pretectum from the basal ganglia to the TeO is well developed (Wilczynski and Northcutt, 1977; Reiner et al., 1980; Wilczynski and Northcutt, 1983; Reiner et al., 1984; Medina and Smeets, 1991; Marín et al., 1997; Reiner et al., 1998). In birds, the pretectal relay station is the SpL. Indeed, the SpL has a prominent GABAergic projection to the ipsilateral TeO (Reiner et al., 1980, 1982a, 1982b, 1984; Veenman, 1997; our results) and shares the connectivity of the SNr (Karten and Dubbledam, 1973; Reiner et al., 1982a; Medina, 1999; Jiao et al., 2000; Reiner et al., 2005). Thus, it is possible that the inhibitory influence of the basal ganglia over the TeO was completely overtaken by this pretectal pathway in birds. Because the SpL–TeO projection is exclusively ipsilateral, it is possible that the nLPT as a caudal extension of the avian SNr emerged to compensate for the nonexistent contralateral projection of the SpL.

An alternative possibility, indicated by the reciprocal connection with the TeO, is that the nLPT could be part of the avian isthmic complex, a compound of several cytoarchitectonically distinguishable nuclei at the mesorhombencephalic border interconnected with the TeO (Hunt et al., 1977; Streit et al., 1980; Yan and Wang, 1986; Güntürkün and Remy, 1990; Woodson et al., 1991; Wang et al., 1995, 2004, 2006; Hellman et al., 2001; Faunes et al., 2013). Although birds possess a highly differentiated isthmic complex, they seem to be the only group among vertebrates that lacks a contralateral projection of this complex (Graybiel, 1978; Sherk, 1979; Roldán et al., 1983; Jen et al., 1984; Künzle and Schnyder, 1984; Baizer et al., 1991; Wiggers and Roth, 1991; Jiang et al., 1996; Johnson et al., 2013). Thus, it cannot be excluded that the nLPT represents the contralaterally projecting component of the avian isthmic complex. In fact, in fish, amphibians, and

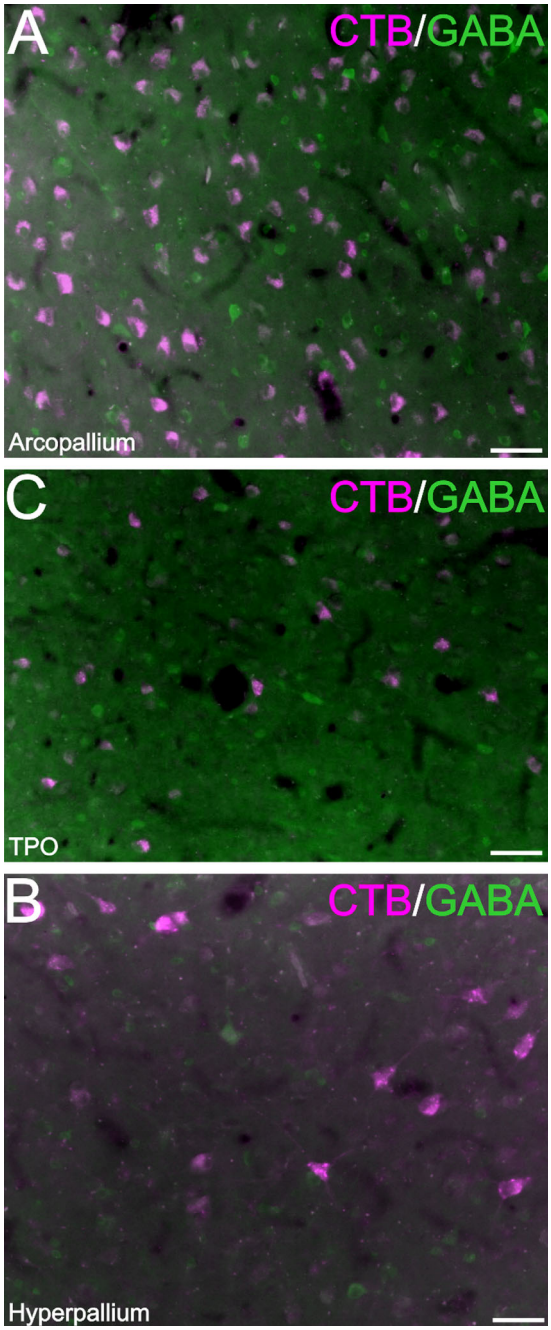

Figure 18. Telencephalic afferents to the optic tectum are not GABAergic. The figure shows sources of telencephalic afferents to the tectum and GABAergic neurons (green) in these regions. Retrogradely labeled neurons (magenta) are observed in the arcopallium (**A**), hyperpallium apicale (**B**), and temporo–parieto–occipital area (TPO) (**C**) after tracer injections into the ipsilateral optic tectum. In all three cases GABAergic neurons and tectally projecting neurons form distinct populations, as no double-labeled neurons were observed in any of these regions. Scale bar = 50 μm in A–C.

mammals the isthmic neurons projecting to the ipsilateral and contralateral TeO occupy different topographical positions within the isthmic nucleus and are even completely separated into distinct nuclei in reptiles (Graybiel, 1978; Sherk, 1979; Roldán et al., 1983; Jen et al., 1984; Künzle and Schnyder, 1984; Baizer et al., 1991; Wiggers and Roth, 1991; Jiang et al., 1996; Johnson et al., 2013). In birds, different isthmic nuclei separated from each other constitute very different connectivity and neurochemistry patterns (Hunt et al., 1977; Streit et al., 1980; Yan and Wang, 1986; Güntürkün and Remy, 1990; Woodson et al., 1991; Medina and Reiner, 1994; Wang et al., 1995, 2004, 2006; Hellman et al., 2001; González-Cabrera et al., 2015). For instance, the magnocellular isthmic nucleus (Imc) is GABAergic (Granda and Crossland, 1989), and its projections to the TeO and other isthmic nuclei are heterotopic and confined to layers 10–12 (Wang et al., 2004). In contrast, the parvocellular nucleus (Ipc) is cholinergic and glutamatergic (Medina and Reiner, 1994; Islam and Atoji, 2008; González-Cabrera et al., 2015) and provides homotopic projections to the TeO throughout layers 2–13 (Wang et al., 2006; González-Cabrera et al., 2016). The cholinergic semilunar nucleus (SLu) provides input to tectal layers 4–11 but also projects to other targets including bilaterally to the nucleus rotundus (Hellmann et al. 2001; Wang et al., 2006). Moreover, in some species, neurons in the Imc that project to the TeO are separated from Imc neurons projecting to the Ipc (Faunes et al., 2013). Thus isthmic neurons with different connectivity patterns tend to form distinct nuclei in birds. Interestingly, the topological position of the nLPT, its tectal connectivity, and its lack of cholinergic neurons (Hunt et al., 1977; Medina and Reiner, 1994) resemble the contralaterally projecting isthmic neurons in reptiles (Künzle and Schnyder, 1984; Sereno and Ulinski, 1987; Powers and Reiner, 1993). The GABAergic nature of the nLPT indicates that nLPT neurons might have demerged from GABAergic neurons of the isthmic complex (Künzle and Schnyder, 1984; Sereno and Ulinski, 1987; Granda and Crossland, 1989; Powers and Reiner, 1993; Wang et al., 2004; Belekhova and Kenigfest, 2014). Therefore, it is conceivable that the nLPT represents a separated population of isthmic neurons that project to the contralateral TeO.

Functional considerations

The idiosyncratic tecto–tectal connectivity pattern of the nLPT suggests that this nucleus could be a key component of interhemispheric communication. Pigeons, like the majority of other birds, have laterally positioned eyes and have a narrow binocular field in comparison with animals with frontally positioned eyes (Güntürkün and Hahmann, 1999; Güntürkün, 2000). Moreover, they preferentially perceive objects in their monocular fields before approaching them (Blough, 1971; Güntürkün, 2000; Ortega et al., 2008). Because the optic fibers of birds cross completely,

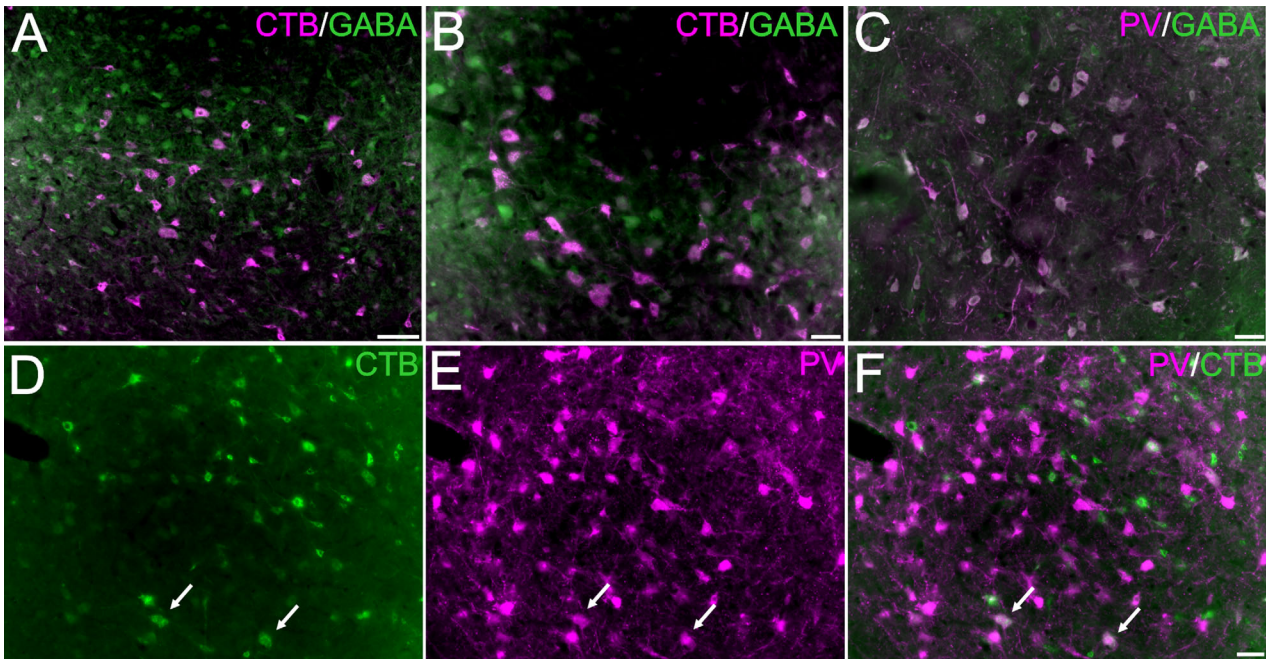

Figure 19. GABA and parvalbumin staining of the substantia nigra, pars reticulata. **A**: CTB-labeled neurons (magenta) in the substantia nigra pars reticulata (SNr) projecting to the ipsilateral tectum and GABAergic neurons of the SNr (green) seem to be distinct populations. **B**: SNr rostral section to A under higher magnification. **C**: Parvalbumin (PV)-expressing neurons (magenta) and GABAergic neurons (green) are colocalized in the SNr. **D–F**: CTB-labeled neurons (green) (D) projecting to the ipsilateral tectum and PV-expressing neurons (magenta) (E) in the SNr. White arrows show double-labeled cells (D and E merged in F). Only two cells were double-labeled. ThusPV-expressing neurons and tectally projecting neurons are also almost completely distinct populations in the SNr. The pictures stem from three different pigeons. Scale bar = 100 μm in A; 50 μm in B, C, and F (also applies to D,E).

each TeO receives virtually different input (Cowan et al., 1961). To avoid potential conflict of the two hemispheres, one hemisphere has to take control and guide response selection, a phenomenon called metacontrol (Adam and Güntürkün, 2009; Ünver and Güntürkün, 2014; Valencia-Alfonso et al., 2009, Freund et al., 2015). Metacontrol could be accomplished by inhibitory projections from one hemisphere to the other (Chiarello and Maxfield, 1996; van der Knaap and van der Ham, 2011). Thus, the GABAergic neurons of the nLPT appear to be suitable candidates for such contralateral inhibition. The left and right TeO could inhibit each other via the nLPT and thus mediate shifts of attentional resources at the cost of the other hemisphere in terms of each one's visual field (Gamlin et al., 1996; Theiss et al., 2003). Our data together with previous evidence suggest that the PT could also be a crucial component in inhibitory intertectal interactions (Gamlin et al., 1996; Karten et al., 1997), but, in contrast to the nLPT, could be more directly involved in ascending visual processing. The PT contains GABAergic neurons (Veenman and Reiner, 1994), projects bilaterally to the TeO, and receives input from the ipsilateral TeO (Gamlin et al., 1996; Karten et al., 1997; present results). Moreover, it is interconnected with the subpretectal nucleus (nSP), which provides GABAergic input to the nucleus rotundus (Mpodozis et al., 1996; Theiss et al., 2003). The nucleus rotundus receives bilateral input from the TeO (Güntürkün et al., 1998). It is possible that the nSP controls a part of the integration of the bilateral information within the ascending visual pathway (Mpodozis et al., 1996; Theiss et al., 2003). Thus the tecto–nLPT–tectal pathway is possibly incorporated in a complex inhibitory interhemispheric network between the bilateral TeO and pretectal and thalamic structures.

These midbrain processes are further modulated by forebrain areas (Valencia-Alfonso et al., 2009; Freund et al., 2015). We found forebrain afferents to the TeO originating in the hyperpallium, arcopallium, and temporo–parieto–occipital area, in accordance with previous studies (Zeier and Karten, 1971; Manns et al., 2007). The hyperpallial top-down afferents were shown to be important in lateralized visual processing (Valencia-Alfonso et al., 2009; Freund et al., 2015). Experiments inactivating the hyperpallium unilaterally demonstrated that these forebrain afferents possibly control the tecto–tectal inhibitory balance (Valencia-Alfonso et al., 2009). Moreover, these afferents seem to be crucial for metacontrol (Freund et al., 2015). A

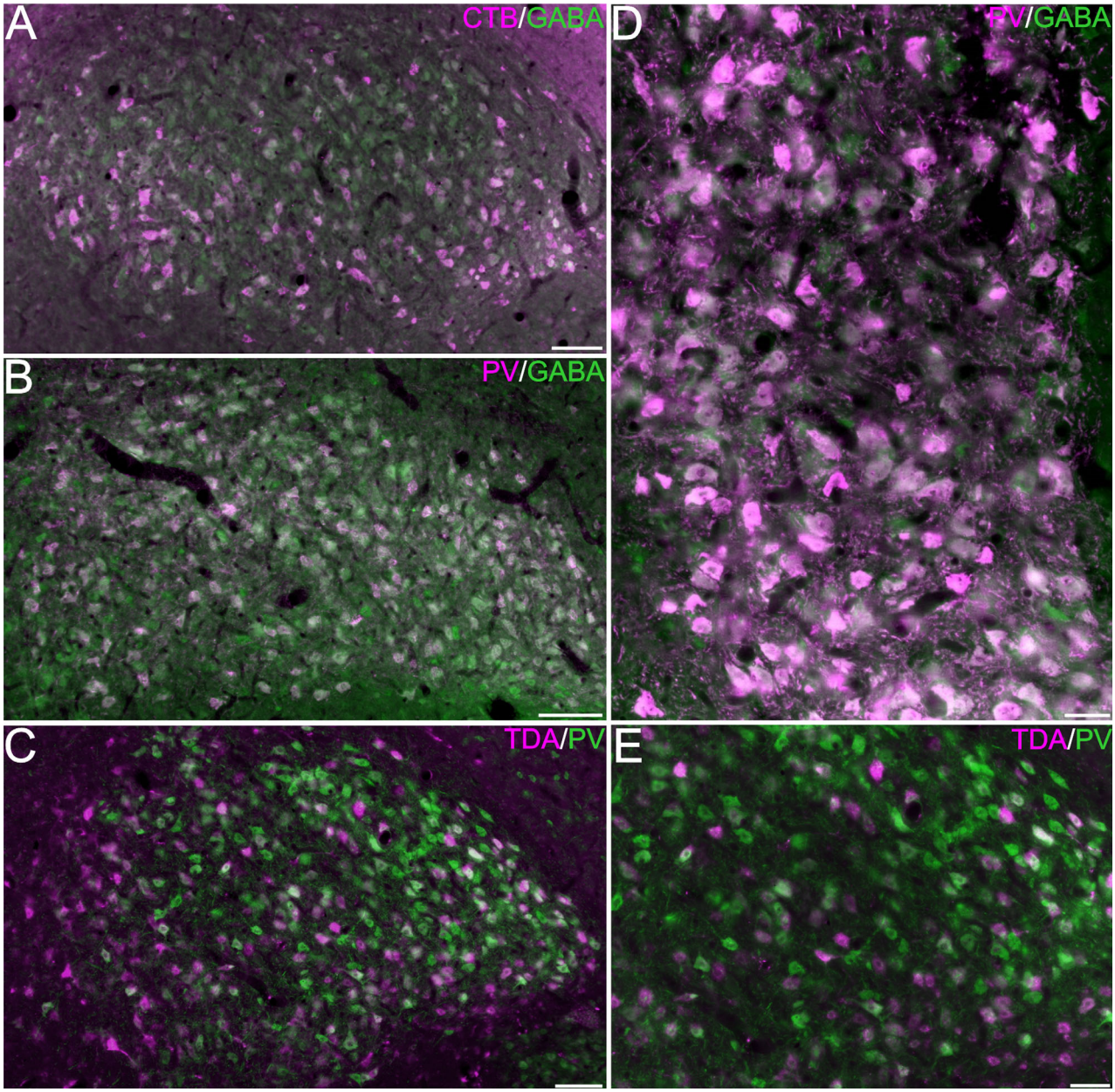

Figure 20. Lateral spiriform nucleus provides GABAergic input to optic tectum. Pictures show the nucleus spiriformis lateralis (SpL) in three different animals. **A**: The vast majority of CTB-labeled SpL neurons, which project to the ipsilateral optic tectum, are GABAergic. **B**: Virtually all parvalbumin-expressing neurons are GABAergic, although some GABAergic neurons are parvalbumin-negative. **C**: Similarly, many TDA-labeled neurons projecting to the ipsilateral tectum coexpress parvalbumin. **D**: Picture of the animal shown in B under higher magnification. **E**: Magnification of C. Scale bar = 100 μm in A–C; 50 μm in D,E.

further key feature of avian vision is the superiority of the left hemisphere for categorization of visual objects based on the discrimination of small features (Güntürkün, 1997; Ocklenburg and Güntürkün, 2012). Because intertectal inhibition is asymmetrically organized, with the left tectum exerting higher interhemispheric inhibition on the right side than vice versa (Keysers et al., 2000), it is conceivable that the nLPT is a nodal point for a functional asymmetry that in pigeons affects homing (Ulrich et al., 1999; Prior et al., 2004; Martinho et al., 2015), pattern discrimination and memorization (Güntürkün, 1985; von Fersen and Güntürkün, 1990), and complex visual cognition (Yamazaki et al., 2007; Manns and Römling, 2012). Thus, the nLPT might be part of an intertectal and forebrain network, which mediates lateralized behavior and hemispheric metacontrol.

Indeed, in mammals, the SNr projection to the contralateral SC was implicated in inhibitory interhemispheric

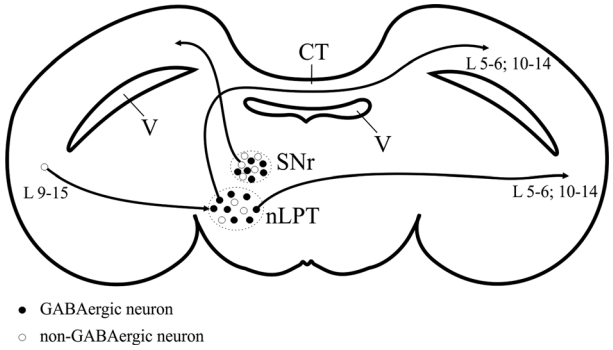

Figure 21. Disynaptic inhibitory tecto–tectal pathway. Intertectal inhibition in pigeons is achieved by GABAergic neurons of the nLPT. Axons of nLPT neurons cross the midline via both the tectal commissura (CT) and the tegmentum. The SNr does not project to the contralateral TeO, and the ipsilateral projection to TeO originates from its non-GABAergic neurons. CT, tectal commissura; L, layer; nLPT, nucleus of the lateral ponto–mesencephalic tegmentum; SNr, substantia nigra pars reticulata; V, ventricle.

interactions (Wallace et al., 1989, 1990; Sprague, 1991; Liu and Basso, 2008). Moreover, Rodríguez et al. (2001) described a deep mesencephalic nucleus in rats, which is located near the substantia nigra and shares its connectivity and physiological properties. They observed a contralateral projection of this nucleus to the SC in addition to a stronger ipsilateral projection. The authors of this study speculate that this nucleus could facilitate interhemispheric interactions.

The possible functional framework of the nLPT would be the same if this nucleus turns out to be part of the isthmic complex (Marín et al., 2007, 2012; Asadollahi et al., 2010; González-Cabrera et al., 2015). In particular, because the isthmic nuclei interact only with the ipsilateral TeO, the nLPT could extend this interaction to the contralateral site. With its projections to layer 10, where the isthmo-tectal neurons are located (Wang et al., 2004, 2006), it could then modulate the isthmo-tectal interaction at the contralateral site and coordinate stimulus attention between the left and right visual fields.

CONCLUSIONS

The starting point of our study was the discrepancy between physiological evidence for a prominent tecto–tectal inhibition and the anatomical sparseness of direct tecto–tectal connections. Searching for an indirect tecto–tectal connection, we detected a new GABAergic tegmental nucleus that could specifically mediate tecto–tectal inhibition. In addition, our study suggests that the pretectal pathway from the basal ganglia to the TeO via the SpL might have overtaken the role of the GABAergic nigrotectal projection during avian evolution.

ACKNOWLEDGMENTS

We thank Sabine Kesch for animal care, Maike Kümper for her assistance during the investigation of the topography of the nLPT, and Felix Ströckens and Rena Klose for providing us with two CTB-injected animals. We also thank Tomas Vega-Zuniga and Harald Luksch for their kind help and support during establishment of the in vitro tracing.

CONFLICT OF INTEREST STATEMENT

The authors declare they have no competing financial, personal, or other interests.

ROLE OF AUTHORS

All authors had full access to all the data in the study and take responsibility for the integrity of the data and the accuracy of the data analysis. Study concept and design: O.G. Acquisition of data: M.S., S.L., C.T. Analysis and interpretation of data: M.S., S.L., M.M., O.G. Drafting of the manuscript: M.S. Critical revision of the manuscript for important intellectual content: M.S., O.G., S.L., M.M., C.T. Obtained funding: O.G. and M.M. Administrative, technical, and material support: O.G., C.T. Study supervision: O.G., S.L.

LITERATURE CITED

Adam R, Güntürkün O. 2009. When one hemisphere takes control: metacontrol in pigeons (*Columba livia*). PLoS One 4:e5307.

Anderson KD, Reiner A. 1991. Striatonigral projection neurons: a retrograde labeling study of the percentages that contain substance P or enkephalin in pigeons. J Comp Neurol 4:658–673.

Araki M, McGeer PL, McGeer EG. 1984. Presumptive gamma-aminobutyric acid pathways from the midbrain to the superior colliculus studied by a combined horseradish peroxidase-gamma-aminobutyric acid transaminase pharmacohistochemical method. Neuroscience 2:433–439.

Asadollahi A, Mysore SP, Knudsen EI. 2010. Stimulus-driven competition in a cholinergic midbrain nucleus. Nat Neurosci 7:889–895.

Baizer JS, Whitney JF, Bender DB. 1991. Bilateral projections from the parabigeminal nucleus to the superior colliculus in monkey. Exp Brain Res 3:467–470.

Beckstead RM, Frankfurter A. 1982. The distribution and some morphological features of substantia nigra neurons that project to the thalamus, superior colliculus and pedunculopontine nucleus in the monkey. Neuroscience 10:2377–2388.

Belekhova MG, Kenigfest NB. 2014. Turtle isthmic complex of visual nuclei: immunohistochemistry of gamma-aminobutyric acid, choline acetyltransferase, calcium-binding proteins and histochemistry of cytochrome oxidase activity. J Evol Biochem Physiol 5:435–447.

Bickford ME, Hall WC. 1992. The nigral projection to predorsal bundle cells in the superior colliculus of the rat. J Comp Neurol 1:11–33.

Blough PM. 1971. The visual acuity of the pigeon for distant targets. J Exp Anal Behav 1:57–67.
Chebat D, Boire D, Ptito M. 2006. Development of the commissure of the superior colliculus in the hamster. J Comp Neurol 6:887–902.
Chiarello C, Maxfield L. 1996. Varieties of interhemispheric inhibition, or how to keep a good hemisphere down. Brain Cogn 1:81–108.
Cowan WM, Adamson L, Powell TP. 1961. An experimental study of the avian visual system. J Anat 95:545–563.
Deniau JM, Chevalier G. 1992. The lamellar organization of the rat substantia nigra pars reticulata: distribution of projection neurons. Neuroscience 2:361–377.
Edwards SB. 1977. The commissural projection of the superior colliculus in the cat. J Comp Neurol 1:23–40.
Ehrlich D, Saleh CN. 1982. Composition of the tectal and posterior commissures of the chick (*Gallus domesticus*). Neurosci Lett 2:115–121.
Ewert JP, Buxbaum-Conradi H, Glagow M, Rottgen A, Schurg-Pfeiffer E, Schwippert WW. 1999. Forebrain and midbrain structures involved in prey-catching behaviour of toads: stimulus-response mediating circuits and their modulating loops. Eur J Morphol 2–3:172-176.
Ewert JP, Buxbaum-Conradi H, Dreisvogt F, Glagow M, Merkel-Harff C, Röttgen A, Schürg-Pfeiffer E, Schwippert W. 2001. Neural modulation of visuomotor functions underlying prey-catching behaviour in anurans: perception, attention, motor performance, learning. Comp Biochem Physiol A 3:417–460.
Faunes M, Fernandez S, Gutierrez-Ibanez C, Iwaniuk AN, Wylie DR, Mpodozis J, Karten HJ, Marin G. 2013. Laminar segregation of GABAergic neurons in the avian nucleus isthmi pars magnocellularis: a retrograde tracer and comparative study. J Comp Neurol 8:1727–1742.
Freund N, Valencia-Alfonso CE, Kirsch J, Brodmann K, Manns M, Güntürkün O. 2015. Asymmetric top-down modulation of ascending visual pathways in pigeons. Neuropsychologia 83:37–47.
Gamlin PD, Reiner A, Keyser KT, Brecha N, Karten HJ. 1996. Projection of the nucleus pretectalis to a retinorecipient tectal layer in the pigeon (*Columba livia*). J Comp Neurol 3:424–438.
Gerfen CR, Baimbridge KG, Miller JJ. 1985. The neostriatal mosaic: compartmental distribution of calcium-binding protein and parvalbumin in the basal ganglia of the rat and monkey. Proc Natl Acad Sci U S A 24:8780–8784.
Gerfen CR, Staines WA, Arbuthnott GW, Fibiger HC. 1982. Crossed connections of the substantia nigra in the rat. J Comp Neurol 3:283–303.
Gonzalez-Cabrera C, Garrido-Charad F, Roth A, Marín GJ. 2015. The isthmic nuclei providing parallel feedback connections to the avian tectum have different neurochemical identities: expression of glutamatergic and cholinergic markers in the chick (*Gallus gallus*). J Comp Neurol 9:1341–1358.
González-Cabrera C, Garrido-Charad F, Mpodozis J, Bolam JP, Marín GJ. 2016. Axon terminals from the nucleus isthmi pars parvocellularis control the ascending retinotectofugal output through direct synaptic contact with tectal ganglion cell dendrites. J Comp Neurol 2:362–379.
Granda RH, Crossland WJ. 1989. GABA-like immunoreactivity of neurons in the chicken diencephalon and mesencephalon. J Comp Neurol 4:455–469.
Graybiel AM. 1978. A satellite system of the superior colliculus: the parabigeminal nucleus and its projections to the superficial collicular layers. Brain Res 2:365–374.
Grofová I, Ottersen OP, Rinvik E. 1978. Mesencephalic and diencephalic afferents to the superior colliculus and periaqueductal gray substance demonstrated by retrograde axonal transport of horseradish peroxidase in the cat. Brain Res 2:205–220.
Grover BG, Sharma SC. 1981. Organization of extrinsic tectal connections in goldfish (*Caraccius auratus*). J Comp Neurol 3:471–488.
Gruberg ER, Kicliter E, Newman EA, Kass L, Hartline PH. 1979. Connections of the tectum of the rattlesnake *Crotalus viridis*: an HRP study. J Comp Neurol 1:31–41.
Güntürkün O. 1985. Lateralization of visually controlled behavior in pigeons. Physiol Behav 4:575–577.
Güntürkün O. 1997. Avian visual lateralization: a review. Neuroreport 6:iii–xi.
Güntürkün O. 2000. Sensory physiology: vision. In: Sturkie's Avian Physiology, 5th ed. San Diego, CA: Academic Press. p 1–19.
Güntürkün O, Böhringer PG. 1987. Lateralization reversal after intertectal commissurotomy in the pigeon. Brain Res 1–2:1-5.
Güntürkün O, Hahmann U. 1999. Functional subdivisions of the ascending visual pathways in the pigeon. Behav Brain Res 2:193–201.
Güntürkün O, Remy M. 1990. The topographical projection of the nucleus isthmi pars parvocellularis (Ipc) onto the tectum opticum in the pigeon. Neurosci Lett 1–2:18-22.
Güntürkün O, Hellmann B, Melsbach G, Prior H. 1998. Asymmetries of representation in the visual system of pigeons. Neuroreport 9:4127–4130.
Hall K, Brauth SE, Kitt CA. 1984. Retrograde transport of 3HGABA in the striatotegmental system of the pigeon. Brain Res 1:157–163.
Hamassaki DE, Britto LR. 1987. Interocular transfer of habituation in pigeons: mediation by tectal and/or posterior commissures. Behav Brain Res 2:175–179.
Hardy O, Leresche N, Jassik-Gerschenfeld D. 1984. Postsynaptic potentials in neurons of the pigeon's optic tectum in response to afferent stimulation from the retina and other visual structures: an intracellular study. Brain Res 1:65–74.
Harting JK, Huerta MF, Hashikawa T, Weber JT, Van Lieshout, D P. 1988. Neuroanatomical studies of the nigrotectal projection in the cat. J Comp Neurol 4:615–631.
Hellmann B, Güntürkün O. 2001. Structural organization of parallel information processing within the tectofugal visual system of the pigeon. J Comp Neurol 429:94–112.
Hellmann B, Manns M, Güntürkün O. 2001. Nucleus isthmi, pars semilunaris as a key component of the tectofugal visual system in pigeons. J Comp Neurol 429:153–166.
Hellmann B, Güntürkün O, Manns M. 2004. Tectal mosaic: organization of the descending tectal projections in comparison to the ascending tectofugal pathway in the pigeon. J Comp Neurol 4:395–410.
Hemsley JP, Savage GE. 1989. Interocular transfer of preoperatively trained visual discriminations in goldfish (*Carassius auratus*) following selective commissure transections. Behav Brain Res 3:297–304.
Herrero L, Perez P, Nunez Abades P, Hardy O, Torres B. 1999. Tectotectal connectivity in goldfish. J Comp Neurol 3:455–471.
Hottman TJ, Sheridan CL, Levinson DM. 1981. Interocular transfer in albino rats as a function of forebrain or forebrain plus midbrain commissurotomy. Physiol Behav 2: 279–285.
Huerta MF, Harting JK. 1984. Connectional organization of the superior colliculus. Trends Neurosci 8:286–289.
Hunt SP, Brecha N. 1984. The avian optic tectum: a synthesis of morphology and biochemistry. In Vanegas H, editor. Comparative neurology of the optic tectum. New York: Plenum Press. p 619–648.

Hunt SP, Künzle H. 1976. Observations on the projections and intrinsic organization of the pigeon optic tectum: an autoradiographic study based on anterograde and retrograde, axonal and dendritic flow. J Comp Neurol 2:153–172.

Hunt SP, Streit P, Künzle H, Cuénod M. 1977. Characterization of the pigeon isthmo-tectal pathway by selective uptake and retrograde movement of radioactive compounds and by Golgi-like horseradish peroxidase labeling. Brain Res 2:197–212.

Ingle D, Campbell A. 1977. Interocular transfer of visual discriminations in goldfish after selective commissure lesions. J Comp Physiol Psychol 2:327–335.

Islam MR, Atoji Y. 2008. Distribution of vesicular glutamate transporter 2 and glutamate receptor 1 mRNA in the central nervous system of the pigeon (*Columba livia*). J Comp Neurol 5:658–677.

Jen LS, Dai ZG, So KF. 1984. The connections between the parabigeminal nucleus and the superior colliculus in the golden hamster. Neurosci Lett 2:189–194.

Jiang ZD, King AJ, Moore DR. 1996. Topographic organization of projection from the parabigeminal nucleus to the superior colliculus in the ferret revealed with fluorescent latex microspheres. Brain Res 1-2:217-232.

Jiao Y, Medina L, Veenman CL, Toledo C, Puelles L, Reiner A. 2000. Identification of the anterior nucleus of the ansa lenticularis in birds as the homolog of the mammalian subthalamic nucleus. J Neurosci 18:6998–7010.

Johnson NP, Schwab TF, Saidel WM. 2013. Bilateral efferents from nucleus isthmi to the optic tectum in goldfish (*Carassius auratus*) are spatially restricted. Neuroscience Lett 534:311–315.

Karten HJ, Cox K, Mpodozis J. 1997. Two distinct populations of tectal neurons have unique connections within the retinotectorotundal pathway of the pigeon (Columba livia). J. Comp. Neurol. 387:449–465.

Karten HJ, Dubbeldam JL. 1973. The organization and projections of the paleostriatal complex in the pigeon (*Columba livia*). J Comp Neurol 1:61–89.

Karten HJ, Hodos W. 1967. A stereotaxic atlas of the brain of the pigeon: *Columba livia*. Baltimore, MD: Johns Hopkins Press Karten. 1997.

Keysers C, Diekamp B, Güntürkün B. 2000. Evidence for physiological asymmetries in the intertectal connections of the pigeon (*Columba livia*) and their potential role in brain lateralisation. Brain Res 2:406–413.

Kitt CA, Brauth SE. 1981. Projections of the paleostriatum upon the midbrain tegmentum in the pigeon. Neuroscience 8:1551–1566.

Kitt CA, Brauth SE. 1986. Telencephalic projections from midbrain and isthmal cell groups in the pigeon. II. The nigral complex. J Comp Neurol 1:92–110.

Knudsen EI. 2011. Control from below: the role of a midbrain network in spatial attention. Eur J Neurosci 11:1961–1972.

Krauzlis RJ, Lovejoy LP, Zénon A. 2013. Superior colliculus and visual spatial attention. Annu Rev Neurosci 36:165–182.

Kuenzel WJ, Medina L, Csillag A, Perkel DJ, Reiner A. 2011. The avian subpallium: new insights into structural and functional subdivisions occupying the lateral subpallial wall and their embryological origins. Brain Res 1424:67–101.

Künzle H, Schnyder H. 1984. The isthmus-tegmentum complex in the turtle and rat: a comparative analysis of its interconnections with the optic tectum. Exp Brain Res 3: 509–522.

Lázár G. 1984. Structure and connections of the frog optic tectum. In Vanegas H, editor. Comparative neurology of the optic tectum. New York: Plenum Press. p 185–210.

Lázár G, Toth P, Csank G, Kicliter E. 1983. Morphology and location of tectal projection neurons in frogs: a study with HRP and cobalt-filling. J Comp Neurol 1:108–120.

Liu P, Basso MA. 2008. Substantia nigra stimulation influences monkey superior colliculus neuronal activity bilaterally. J Neurophysiol 2:1098–1112.

Luksch H. 2003. Cytoarchitecture of the avian optic tectum: neuronal substrate for cellular computation. Rev Neurosci 1–2:85-106.

Luque AM, Pilar Pérez-Pérez M, Herrero L, Torres B. 2005. Involvement of the optic tectum and mesencephalic reticular formation in the generation of saccadic eye movements in goldfish. Brain Res Rev 2:388–397.

Manns M, Römling J. 2012. The impact of asymmetrical light input on cerebral hemispheric specialization and interhemispheric cooperation. Nat Commun 3:696.

Manns M, Freund N, Patzke N, Güntürkün O. 2007. Organization of telencephalotectal projections in pigeons: impact for lateralized top-down control. Neuroscience 2:645–653.

Marín O, González A, Smeets WJ. 1997. Basal ganglia organization in amphibians: efferent connections of the striatum and the nucleus accumbens. J Comp Neurol 1:23–50.

Marín O, González A, Smeets WJ. 1997. Basal ganglia organization in amphibians: efferent connections of the striatum and the nucleus accumbens. J Comp Neurol 1:23–50.

Marín G, Letelier JC, Henny P, Sentis E, Farfan G, Fredes F, Pohl N, Karten H, Mpodozis J. 2003. Spatial organization of the pigeon tectorotundal pathway: an interdigitating topographic arrangement. J Comp Neurol 4:361–380.

Marín G, Salas C, Sentis E, Rojas X, Letelier JC, Mpodozis J. 2007. A cholinergic gating mechanism controlled by competitive interactions in the optic tectum of the pigeon. J Neurosci 30:8112–8121.

Marín GJ, Duran E, Morales C, Gonzalez-Cabrera C, Sentis E, Mpodozis J, Letelier JC. 2012. Attentional capture? Synchronized feedback signals from the isthmi boost retinal signals to higher visual areas. J Neurosci 3:1110–1122.

Mark RF. 1966. The tectal commissure and interocular transfer of pattern discrimination in cichlid fish. Exp Neurol 2: 215–225.

Martinho A, Biro D, Guilford T, Gagliardo A, Kacelnik A. 2015. Asymmetric visual input and route recapitulation in homing pigeons. Proc R Soc B 282.

Mascetti GG, Arriagada JR. 1981. Tectotectal interactions through the commissure of the superior colliculi: an electrophysiological study. Exp Neurol 1:122–133.

May PJ, Hall WC. 1986. The sources of the nigrotectal pathway. Neuroscience 1:159–180.

McRitchie DA, Hardman CD, Halliday GM. 1996. Cytoarchitectural distribution of calcium binding proteins in midbrain dopaminergic regions of rats and humans. J Comp Neurol 1:121–150.

Medina L, Reiner A, Jiao Y. 1999. The Functional Anatomy of the Basal Ganglia of Birds. Eur J Morphol 37:160–165.

Medina L, Reiner A. 1994. Distribution of choline acetyltransferase immunoreactivity in the pigeon brain. J Comp Neurol 4:497–537.

Medina L, Reiner A. 1997. The efferent projections of the dorsal and ventral pallidal parts of the pigeon basal ganglia, studied with biotinylated dextran amine. Neuroscience 3: 773–802.

Medina L, Smeets WJ. 1991. Comparative aspects of the basal ganglia-tectal pathways in reptiles. J Comp Neurol 4:614–629.

Medina L, Veenman CL, Reiner A. 1997. Evidence for a possible avian dorsal thalamic region comparable to the mammalian ventral anterior, ventral lateral, and oral ventroposterolateral nuclei. J Comp Neurol 1:86–108.

Medina L, Jiao Y, Reiner A. 1999. The functional anatomy of the basal ganglia of birds. Eur J Morphol 2-3:160-165.

Mpodozis J, Cox K, Shimizu T, Bischof HJ, Woodson W, Karten HJ. 1996. GABAergic inputs to the nucleus rotundus (pulvinar inferior) of the pigeon (*Columba livia*). J Comp Neurol 2:204–222.

Mysore SP, Knudsen EI. 2011. The role of a midbrain network in competitive stimulus selection. Curr Opin Neurobiol 4: 653–660.

Niida A. 1973. Visual responses from ipsilateral optic tectum of crucian carp. Journal of the Faculty of Science Hokkaido University Series VI. Zoology 1:50–57.

Northcutt RG. 1982. Localization of neurons afferent to the optic tectum in longnose gars. J Comp Neurol 4:325–335.

Northcutt RG. 1984. Anatomical organization of the optic tectum in reptiles. In Vanegas H, editor. Comparative neurology of the optic tectum. New York: Plenum Press. p 547–600.

Ocklenburg S, Güntürkün O. 2012. Hemispheric asymmetries: the comparative view. Front Psychol 3:5.

Ortega LJ, Stoppa K, Güntürkün O, Troje NF. 2008. Limits of intraocular and interocular transfer in pigeons. Behav Brain Res 1:69–78.

Peck CK, Crewther SG, Hamilton CR. 1979. Partial interocular transfer of brightness and movement discrimination by split-brain cats. Brain Res 1:61–75.

Pérez-Santana L, Martinez-de-la-Torre M, Loro JF, Puelles L. 1996. Intertectal commissural projection in the lizard *Gallotia stehlini*: origin and midline topography. J Comp Neurol 2:360–369.

Powers SA, Reiner A. 1993. The distribution of cholinergic neurons in the central nervous system of turtles. Brain Behav Evol 6:326–345.

Prior H, Wiltschko R, Stapput K, Güntürkün O, Wiltschko W. 2004. Visual lateralization and homing in pigeons. Behav Brain Res 2:301–310.

Reiner A, Anderson KD. 1993. Co-occurrence of gamma-aminobutyric acid, parvalbumin and the neurotensin-related neuropeptide LANT6 in pallidal, nigral and striatal neurons in pigeons and monkeys. Brain Res 1–2:317-325.

Reiner A, Karten HJ. 1982. Laminar distribution of the cells of origin of the descending tectofugal pathways in the pigeon (*Columba livia*). J Comp Neurol 2:165–187.

Reiner A, Brauth SE, Kitt CA, Karten HJ. 1980. Basal ganglionic pathways to the tectum: studies in reptiles. J Comp Neurol 2:565–589.

Reiner A, Brecha NC, Karten HJ. 1982a. Basal ganglia pathways to the tectum: the afferent and efferent connections of the lateral spiriform nucleus of pigeon. J Comp Neurol 1:16–36.

Reiner A, Karten HJ, Brecha NC. 1982b. Enkephalin-mediated basal ganglia influences over the optic tectum: immunohistochemistry of the tectum and the lateral spiriform nucleus in pigeon. J Comp Neurol 1:37–53.

Reiner A, Karten HJ, Solina AR. 1983. Substance P: localization within paleostriatal-tegmental pathways in the pigeon. Neuroscience 1:61–85.

Reiner A, Brauth SE, Karten HJ. 1984. Evolution of the amniote basal ganglia. Trends Neurosci 9:320–325.

Reiner A, Medina L, Veenman CL. 1998. Structural and functional evolution of the basal ganglia in vertebrates. Brain Res Brain Res Rev 3:235–285.

Reiner A, Perkel DJ, Bruce LL, Butler AB, Csillag A, Kuenzel W, Medina L, Paxinos G, Shimizu T, Striedter G, Wild M, Ball GF, Durand S, Güntürkün O, Lee DW, Mello CV, Powers A, White SA, Hough G, Kubikova L, Smulders TV, Wada K, Dugas-Ford J, Husband S, Yamamoto K, Yu J, Siang C, Jarvis ED. 2004. Revised nomenclature for avian telencephalon and some related brainstem nuclei. J Comp Neurol 3:377–414.

Reiner A, Yamamoto K, Karten HJ. 2005. Organization and evolution of the avian forebrain. Anat Rec A Discov Mol Cell Evol Biol 1:1080–1102.

Rhoades RW, Mooney RD, Szczepanik AM, Klein BG. 1986. Structural and functional characteristics of commissural neurons in the superior colliculus of the hamster. J Comp Neurol 2:197–215.

Rhoades RW, Fish SE, Voneida TJ. 1981. Anatomical and electrophysiological demonstration of tectotectal pathway in the golden hamster. Neurosci Lett 3:255–260.

Rinvik E, Grofová I, Ottersen OP. 1976. Demonstration of nigrotectal and nigroreticular projections in the cat by axonal transport of proteins. Brain Res 2:388–394.

Robert F, Cuénod M. 1969a. Electrophysiology of the intertectal commissures in the pigeon. I. Analysis of the pathways. Exp Brain Res 2:116–122.

Robert F, Cuénod M. 1969b. Electrophysiology of the intertectal commissures in the pigeon. II. Inhibitory interaction. Exp Brain Res 2:123–136.

Rodman HR, Karten HJ. 1995. Laminar distribution and sources of catecholaminergic input to the optic tectum of the pigeon (*Columbia livia*). J Comp Neurol 3:424–442.

Rodríguez M, Abdala P, Barroso-Chinea P, Gonzalez-Hernandez T. 2001. The deep mesencephalic nucleus as an output center of basal ganglia: morphological and electrophysiological similarities with the substantia nigra. J Comp Neurol 1:12–31.

Roldán M, Reinoso-Suarez F, Tortelly A. 1983. Parabigeminal projections to the superior colliculus in the cat. Brain Res 1:1–13.

Sereno MI, Ulinski PS. 1987. Caudal topographic nucleus isthmi and the rostral nontopographic nucleus isthmi in the turtle, *Pseudemys scripta*. J Comp Neurol 3:319–346.

Sherk H. 1979. Connections and visual-field mapping in cat's tectoparabigeminal circuit. J Neurophysiol 6:1656–1668.

Sherman SM. 1974. Visual fields of cats with cortical and tectal lesions. Science 4148:355–357.

Shu SY, Ju G, Fan LZ. 1988. The glucose oxidase-DAB-nickel method in peroxidase histochemistry of the nervous system. Neurosci Lett 2:169–171.

Smeets WJ. 1981. Efferent tectal pathways in two chondrichthyans, the shark *Scyliorhinus canicula* and the ray *Raja clavata*. J Comp Neurol 1:13–23.

Sparks DL, Mays LE. 1990. Signal transformations required for the generation of saccadic eye movements. Annu Rev Neurosci 13:309–336.

Sprague JM. 1991. The role of the superior colliculus in facilitating visual attention and form perception. Proc Natl Acad Sci U S A 4:1286–1290.

Stephenson-Jones M, Ericsson J, Robertson B, Grillner S. 2012. Evolution of the basal ganglia: dual-output pathways conserved throughout vertebrate phylogeny. J Comp Neurol 13:2957–2973.

Streit P, Knecht E, Cuenod M. 1980. Transmitter-related retrograde labeling in the pigeon optic lobe: a high resolution autoradiographic study. Brain Res 1:59–67.

Tardif E, Clarke S. 2002. Commissural connections of human superior colliculus. Neuroscience 2:363–372.

Theiss MP, Hellmann B, Güntürkün O. 2003. The architecture of an inhibitory sidepath within the avian tectofugal system. Neuroreport 6:879–882.

Ulrich C, Prior H, Duka T, Leshchins'ka I, Valenti P, Güntürkün O, Lipp HP. 1999. Left-hemispheric superiority for visuospatial orientation in homing pigeons. Behav Brain Res 1–2:169-178.

Ünver E, Güntürkün O. 2014. Evidence for interhemispheric conflict during meta-control in pigeons. Behav Brain Res 270:146–150.

Valencia-Alfonso C, Verhaal J, Güntürkün O. 2009. Ascending and descending mechanisms of visual lateralization in pigeons. Philos Trans R Soc Lond B Biol Sci 1519:955–963.

van der Knaap LJ, van der Ham IJ. 2011. How does the corpus callosum mediate interhemispheric transfer? A review. Behav Brain Res 1:211–221.

Veenman CL. 1997. Pigeon basal ganglia: insights into the neuroanatomy underlying telencephalic sensorimotor processes in birds. Eur J Morphol 4:220–233.

Veenman CL, Reiner A. 1994. The distribution of GABA-containing perikarya, fibers, and terminals in the forebrain and midbrain of pigeons, with particular reference to the basal ganglia and its projection targets. J Comp Neurol 2:209–250.

von Fersen L, Güntürkün O. 1990. Visual memory lateralization in pigeons. Neuropsychologia 1:1–7.

Voneida TJ, Mello NK. 1975. Interhemispheric projections of the optic tectum in pigeon. Brain Behav Evol 2:91–108.

Wallace SF, Rosenquist AC, Sprague JM. 1989. Recovery from cortical blindness mediated by destruction of nontectotectal fibers in the commissure of the superior colliculus in the cat. J Comp Neurol 3:429–450.

Wallace SF, Rosenquist AC, Sprague JM. 1990. Ibotenic acid lesions of the lateral substantia nigra restore visual orientation behavior in the hemianopic cat. J Comp Neurol 2:222–252.

Wang SR, Wang YC, Frost BJ. 1995. Magnocellular and parvocellular divisions of pigeon nucleus isthmi differentially modulate visual responses in the tectum. Exp Brain Res 3:376–384.

Wang Y, Luksch H, Brecha NC, Karten HJ. 2006. Columnar projections from the cholinergic nucleus isthmi to the optic tectum in chicks (*Gallus gallus*): a possible substrate for synchronizing tectal channels. J Comp Neurol 1:7–35.

Wang Y, Major DE, Karten HJ. 2004. Morphology and connections of nucleus isthmi pars magnocellularis in chicks (*Gallus gallus*). J Comp Neurol 2:275–297.

Welker E, Hoogland PV, Lohman AH. 1983. Tectal connections in *Python reticulatus*. J Comp Neurol 3:347–354.

Wiggers W, Roth G. 1991. Anatomy, neurophysiology and functional aspects of the nucleus isthmi in salamanders of the family Plethodontidae. J Comp Physiol A 2: 165–176.

Wilczyniski W, Northcutt RG. 1977. Afferents to the optic tectum of the leopard frog: an HRP study. J Comp Neurol 2: 219–230.

Wilczynski W, Northcutt RG. 1983. Connections of the bullfrog striatum: efferent projections. J Comp Neurol 3: 333–343.

Woodson W, Reiner A, Anderson K, Karten HJ. 1991. Distribution, laminar location, and morphology of tectal neurons projecting to the isthmo-optic nucleus and the nucleus isthmi, pars parvocellularis in the pigeon (*Columba livia*) and chick (*Gallus domesticus*): a retrograde labelling study. J Comp Neurol 3:470–488.

Wurtz RH. 2009. Superior colliculus. In Squire L, editor. Encyclopedia of neuroscience. Oxford, UK: Elsevier, Academic Press.

Wylie DRW, Gutierrez-Ibanez C, Pakan, JM, Iwaniuk AN. 2009. The optic tectum of birds: mapping our way to understanding visual processing. Can J Exp Psychol 4: 328–338.

Yamasaki DS, Krauthamer G, Rhoades RW. 1984. Organization of the intercollicular pathway in rat. Brain Res 2:368–371.

Yamazaki Y, Aust U, Huber L, Hausmann M, Güntürkün O. 2007. Lateralized cognition: asymmetrical and complementary strategies of pigeons during discrimination of the "human concept". Cognition 2:315–344.

Yan K, Wang SR. 1986. Visual responses of neurons in the avian nucleus isthmi. Neurosci Lett 3:340–344.

Zeier H, Karten HJ. 1971. The archistriatum of the pigeon: organization of afferent and efferent connections. Brain Res 2:313–326.